8-2008

A Spectroscopic Analysis of HD 134439 and HD 134440

Yu Chen
Clemson University, yuc@clemson.edu

A Spectroscopic Analysis of HD 134439 and HD 134440

A Thesis
Presented to
the Graduate School of
Clemson University

In Partial Fulfillment
of the Requirements for the Degree
Master of Science
Physics

---

by
Yu Chen
December 2008

Accepted by:
Dr. Jeremy R. King, Committee Chair
Dr. Bradley S. Meyer
Dr. Sean D. Brittain

Abstract

We analyze elemental abundances of the common proper motion pair HD 134439 and HD 134440 to understand their formation history. This pair of metal-poor ([Fe/H]~ -1.50) halo dwarfs are known, from previous studies, to exhibit abnormally low [α/Fe] ratios compared to typical Galactic halo stars. Some have attributed this to planetesimal accretion; others believe these stars formed in the dusty part of a dwarf spheroidal galaxy and were later captured by our Galaxy. To investigate this anomaly, we measure carbon, nitrogen, and oxygen abundances for HD 134439 and HD 134440 from near-UV molecular features using high-resolution spectra obtained with Keck HIRES spectrograph. The [C, N, O/Fe] ratios range from ~ -0.30 to ~ -0.60 dex. We confirm a previously suggested correlation between the elemental abundances and condensation temperature at the $\sim$5% confidence level. A comparison of HD 134439 and HD 134440 with stars of similar metallicity in the Galactic halo suggests very different formation histories; though, the abundances of dwarf spheroidal stars seems less different from our stars. Chemical yields of low mass Type II supernovae provide an explanation for most of the abundance patterns observed for the common proper motion pair. Finally, the peculiar abundances of neutron-capture elements (Y, Ag, Ba, Eu) are put in context with various nucleosynthetic sources.

Dedication

This thesis is dedicated to my family. I am grateful for their support and encouragement throughout my life.

Acknowledgments

First and foremost, I would like to thank Dr. Jeremy King for his advice throughout my graduate career. I am very honored to have him as my research advisor. My gratitude also goes to Dr. Bradley Meyer and Dr. Sean Brittain for serving as my committee.

I am very thankful for all the knowledge Eric has shared with me, and for his patience with my repeated questions. Thanks to Roggie and Allen for their help with computers and script writings. Thanks to Simon for sharing his line list and for being a role model.

I thank all my fellow colleagues for their inspirations. A special thanks to Ginger for being my best friend and roommate. Her cheerfulness and encouragement always motivate me. I thank Joe, Matt, Brian, Blake, Russell, Autumn and the whole Physics and Astronomy community for enhancing my experience here at Clemson.

I am also especially grateful to Kang who always provides me with love and support.

Table of Contents

List of Tables

List of Figures

Chapter 1

Introduction

The formation history of the Milky Way remains an enigma that fascinates and puzzles theorists and observers alike. Ongoing developments in stellar and Galactic models improve our understanding of the complex nature of the Galactic origin. Stellar observations are employed to test and constrain these model predictions. The Galaxy has nurtured many generations of stars, some of which have long been dead – e.g. population III stars. This makes direct observation of the entire Galactic history an impossible mission. However, an examination of the current generation stars can provide insight into the nature of their predecessors. The processed chemical products inherited by stars from previous generations can be revealed through stellar spectroscopy.

1.1 Monolithic Collapse Model

In 1962, a rapid monolithic collapse model for the formation of the Galaxy was suggested by Eggen et al. (1962, hereafter ELS) based on their observation of stellar kinematics. They describe a protogalaxy condensing out of a gas cloud on the free-fall timescale of a few hundred million years. The collapse ceases as the inward gravity is equilibrated by the rotation of the Galactic disk. Thus, the end product of the collapse is a rotating disk with a spherical central bulge and an older halo. The increase in gas density during the

condensation provokes initial star formation. This first generation of stars is believed to be: extremely metal-poor ([Fe/H][1] $\lesssim -3$) due to their low metallicity birth environment; typically very massive ($\sim 10^2 M_\odot$) because of inefficient cooling from the lack of metals in the primordial gas; and, thus, short-lived. The kinematics of these first stars are highly eccentric, since they form during early condensation before the system has stabilized. As the extremely metal-poor stars evolve, they produce progressively heavier elements through nuclear burning in their cores. These nucleosynthetic products will enrich the interstellar medium through feedback such as mass loss via stellar winds or stellar explosions. Subsequent stars formed in the chemically enriched environment will inherit elemental signatures of their progenitors.

1.2 Stellar Nucleosynthesis

Stellar nucleosynthesis predicts the chemical processes occurring in various stellar environments. Elements including O, Ne, Mg, Si, S, Ca, and Ti are produced by capture of α particles ($^4_2$He nuclei) at high temperature – e.g., cores of massive stars. For example,

$$^{12}_{6}\mathrm{C} + ^{4}_{2}\mathrm{He} \longrightarrow ^{16}_{8}\mathrm{O} + \gamma, \tag{1.2.1}$$

$$^{16}_{8}\mathrm{O} + ^{4}_{2}\mathrm{He} \longrightarrow ^{20}_{10}\mathrm{Ne} + \gamma. \tag{1.2.2}$$

Iron, when number of neutrons equals number of protons, is the most bound element produced by exothermic nuclear fusion reactions in a stellar interior. Metals heavier than Fe are primarily created by neutron-capture processes that can take place in lower temperature environments. The process requires capturing free neutrons

$$^{A}_{Z}\mathrm{X} + \mathrm{n} \longrightarrow ^{\mathrm{A+1}}_{\mathrm{Z}}\mathrm{X} + \gamma \tag{1.2.3}$$

[1] [Fe/H] indicates the metallicity of a star compared to the Sun

to produce heavier isotopes, which can then β-decay ($n \longrightarrow p^+ + e^- + \bar{\nu}_e$)

$$ {}^{A+1}_{Z}\mathrm{X} \longrightarrow {}^{\mathrm{A+1}}_{\mathrm{Z+1}}\mathrm{X} + \mathrm{e}^- + \bar{\nu}_\mathrm{e} + \gamma. \tag{1.2.4} $$

If the neutron-capture rate is fast compared to β-decay, the resulting reaction is known as the *r*-process. In contrast, the *s*-process corresponds to a slow neutron-capture rate compared to β-decay, which produces nuclei that are more stable. While the *s*-process can occur in low neutron density ($\sim 10^8 \mathrm{cm}^{-3}$; Käppeler et al., 1989) environments, the *r*-process requires high neutron densities ($\sim 10^{19} \mathrm{cm}^{-3}$; Meyer, 1994). Most of the heavy *s*-process nuclei ($A > 90$) are produced in low and intermediate mass (LIM, $0.8M_\odot < M < 8M_\odot$) asymptotic giant branch (AGB) stars, where the neutron density is relatively low. Massive stars that end their lives as core-collapse supernovae, Type II ($8M_\odot < M < 40M_\odot$) or Type Ib/c ($M > 40M_\odot$), produce primarily α-elements (Matteucci, 2008b, and references therein). They are also responsible for making light *s*-process nuclei ($A < 90$), *r*-process nuclei (a result of the neutron rich explosion site), and some Fe. The majority of Fe in the Galaxy, however, is produced by Type Ia supernovae via C-deflagration as a white dwarf reaches its Chandrasekhar mass limit by accreting material from its companion star (e.g., Matteucci, 2008a).

1.3 Galactic Chemical Evolution as Predicted by ELS Model

The Galactic halo, when young, consisted mainly of massive metal-poor stars ($M \sim 10^2 M_\odot$, [Fe/H]$\lesssim -3$) that were formed during the early stage of ELS collapse. When these short-lived massive stars died as core-collapse supernovae, they ejected nucleosynthetic products (abundant in α-elements, but including some Fe) back into the interstellar medium. The next generation of stars formed in this environment carried an overabundance of α-elements. The short burst of star formation in the halo was followed by a rapid density decrease. The subsequent reduced star formation caused the rate of stellar feedback to diminish and the metallicity to increase very slowly.

In the young disk, however, ongoing star formation increases the metallicity at a much faster rate. Type Ia SNe are the greatest contributors to metal enrichment in the disk. However, it takes a LIM star on the order of $\geq 10^9$ years to evolve and then explode as Type Ia supernova, creating a time-delayed injection of Fe into the interstellar medium. This results in an apparent decline of relative [α/Fe] ratios at later times. The continuing build up of metallicity over time in the Galaxy gives rise to an age-metallicity relation – young disk stars are relatively metal-rich compared to the old, and thus metal poor, halo stars (Twarog, 1980).

If the Galactic halo is formed exclusively according to the ELS rapid monolithic collapse model, then the stars observed in halo should exhibit relatively high [α/Fe][2] ratios compared to the Sun. However, stars have been observed with chemical abundances that deviate from this expectation, suggesting an alternative view of the evolutionary history of the Galaxy. An example is shown in Appendix A, the preprint of a paper that will be submitted to The Astronomical Journal. In this manuscript, we investigate a metal-poor common proper motion pair – HD 134439 and HD 134440 – whose elemental abundances are anomalous in comparison to typical halo stars. A concise summary of the results discussed in the paper is present in Chapter 2, along with supplemental materials in Appendix B.

[2] [X/Fe] $\equiv \log \frac{N(\mathrm{X})}{N(\mathrm{H})}_{\star} - \log \frac{N(\mathrm{X})}{N(\mathrm{H})}_{\odot}$ −[Fe/H] where we assume $\log N(\mathrm{H}) = 12.0$

Chapter 2

Results and Future Work

2.1 Abundance Analysis

A detailed analysis of the elemental abundances for HD 134439 and HD 134440 is carried out to understand the origin of these low-α metal-poor halo dwarfs. In particular, we derive new carbon, nitrogen, and oxygen abundances from near-UV electronic molecular lines. Syntheses for various spectral regions are shown in Figures A.1−A.3 of the accompanying paper. We provide additional NH and OH syntheses in Figures B.1−B.3 which are not shown in the paper.

Derived abundances are listed in Tables A.3−A.5, and summarized in Table A.7. We find that relative [C, N, O/Fe] ratios are underabundant compared to typical halo stars. Furthermore, our results (Figure A.4) indicate a trend of decreasing abundance with lower condensation temperature (T_c) at the $\sim$5% confidence level – a behavior previously explained by Shigeyama & Tsujimoto's (2003) planetesimal accretion theory and separately by Chen & Zhao's (2006) hypothesis of a dusty proto-stellar environment in the dwarf spheroidal (dSph) galaxies.

We compare abundances of HD 134439 and HD 134440 to stars of similar metallicity in different systems – i.e., the Galactic halo and dSph galaxies. The abundance differences between our stars and the Galactic halo are correlated with T_c at $< 1\%$ significance level

(Figure A.5). On the other hand, the correlation of HD 134439/440−dSph abundance differences with T_c is only significant at $> 30\%$ (Figure A.8). Thus, if the T_c-related trend is causal, it is likely that HD 134439 and 134440 were formed in an environment more dusty than one the Galactic halo is able to provide. The less apparent difference compared to dSph stars suggests the unlikelihood of an abnormally dusty environment in dSph galaxies as the birth site for our stars.

Further investigation indicates the T_c-related behavior can be illusory, and the abundance pattern observed in HD 134439 and 134440 can be explained by nucleosynthesis. Specifically, we demonstrate the abundances can be due to the chemical enrichment from low mass ($\sim 14 M_\odot$) Type II SNe progenitors. Note these have been invoked to explain abundance ratios in dSph stars. So, kinematics and abundances give consistent picture of an accreted dSph binary.

We have also measured abundances of a few neutron-capture elements – specifically Ag and Eu. The supplemental Ag I syntheses for HD 134440 are shown in Figure B.4. Measurements of [Ag/Fe]~ -0.16 and [Eu/Fe]$\lesssim +0.37$ are obtained for our stars. These abundance ratios are consistently lower in HD 134439 and HD 134440 than other halo stars with similar metallicity. We believe this might have something to do with Qian & Wasserburg's (2001) L class Type II SNe productions. The L class events are related to lower mass Type II supernovae – consistent with our previous conclusions derived from the abundances of other elements. Woosley & Hoffman's (1992) calculations for the α-rich freeze-out yields provide an alternative explanation for the n-element abundances. Their calculations which show over-production of Ti relative to other α-elements was also able to explain the high [Ti/Fe] observed in our stars.

2.2 Future Work

In this work, we were only able to obtain rough estimates for silver abundances and upper limits for europium. Further modifications of the line list could lead to better

abundance estimates from the syntheses. Abundance measurements for more neutron-capture elements (especially heavier elements) would also be beneficial in constraining the nature of r-process elements in HD 134439 and 134440. Also, α-rich freeze-out calculations for A$>$ 47 are needed to identify any observable abundance characteristics to test α-rich freeze-out origin.

Appendices

Appendix A

The following article will be submitted to Astronomical Journal.

A SPECTROSCOPIC ANALYSIS OF HD 134439 and HD 134440

Yu Chen

Department of Physics and Astronomy, Clemson University, Clemson, SC 29630-0978

yuc@clemson.edu

Jeremy R. King

Department of Physics and Astronomy, Clemson University, Clemson, SC 29630-0978

jking2@ces.clemson.edu

and

Ann M. Boesgaard

Institute for Astronomy, 2680 Woodlawn Drive, Honolulu, HI 96822

boes@ifa.hawaii.edu

ABSTRACT

We analyze elemental abundances of the common proper motion pair HD 134439 and HD 134440 to understand their formation history. This pair of metal-poor ([Fe/H]~ -1.50) halo dwarfs are known, from previous studies, to exhibit abnormally low [α/Fe]

ratios compared to typical Galactic halo stars. Some have attributed this to planetesimal accretion; others believe these stars formed in the dusty part of a dwarf spheroidal galaxy and were later captured by our Galaxy. To investigate this anomaly, we measure carbon, nitrogen, and oxygen abundances for HD 134439 and HD 134440 from near-UV molecular features using high-resolution spectra obtained with Keck HIRES spectrograph. The [C, N, O/Fe] ratios range from ~ -0.30 to ~ -0.60 dex. We confirm a previously suggested correlation between the elemental abundances and condensation temperature at the $\sim$5% confidence level. A comparison of HD 134439 and HD 134440 with stars of similar metallicity in the Galactic halo suggests very different formation histories; though, the abundances of dwarf spheroidal stars seems less different from our stars. Chemical yields of low mass Type II supernovae provide an explanation for most of the abundance patterns observed for the common proper motion pair. Finally, the peculiar abundances of neutron-capture elements (Y, Ag, Ba, Eu) are put in context with various nucleosynthetic sources.

Subject headings: stars: metal-poor - stars: abundances - Galaxy: evolution - Galaxy: halo - galaxies: dwarf spheroidal

A.1 INTRODUCTION

The outcome of the Eggen et al. (1962) rapid monolithic collapse (hereafter ELS) model is an old metal-poor Galactic halo with enhanced [α/Fe][1,2] values, and a young metal-rich disk with no enhancement in [α/Fe]. The relative [α/Fe] ratios in stars diminish as a function of Galactic time evolution as metallicity increases from stellar feedbacks. However, stars in the Galaxy do not strictly follow the simple trend expected by ELS model. Carney et al. (1997) reported the low metallicity ([Fe/H]$= -1.86$) star, BD+80°245, as having an abnormally low average [α/Fe] ratio of -0.29 dex. CS 22966-043, a blue metal-poor SX Phe variable star, was also found to exhibit unusual α-element deficiencies (Preston & Sneden, 2000). Other examples include Nissen & Schuster's (1997) sample of

[1] α indicates elements produced by capture of α particles: e.g., O, Ne, Mg, Si, S, Ca, Ti.

[2] [X/Fe]$\equiv \log \frac{N(\mathrm{X})}{N(\mathrm{H})}_{\star} - \log \frac{N(\mathrm{X})}{N(\mathrm{H})}_{\odot} -$[Fe/H] where we assume $\log N(\mathrm{H}) = 12.0$

low α halo stars with large apogalactocentric distances, Brown et al.'s (1997) study on young globular clusters Rup 106 and Pal 12, and King's (1997a) abundance analysis of the halo common proper motion pair HD 134439 and HD 134440. Such objects suggest that an alternative formation mechanism of the Galactic halo is needed to explain these intricate abundance patterns.

Galactic globular clusters are believed to have formed during the rapid condensation of the protogalaxy ($\sim 10^8$ years). If the current Galaxy is a product of rapid monolithic collapse, then the age of the globular clusters should be similar and the age difference should not exceed the collapse time. However, this is contrary to Searle & Zinn's (1978) findings. By examining color-magnitude diagrams of globular clusters in the Galactic halo, they found a diverse horizontal-branch morphology that corresponds to an age spread on the order of 10^9 years, suggesting the formation timescale lasted longer than the free-fall time. Consequently, they suggest the outer halo of the Galaxy could be a product of an accretion of discrete fragments that formed independently of the Galactic collapse. The accretion events could very likely extend more than 1 Gyr.

Prantzos (2007) showed that the halo metallicity distribution is very well reproduced by the merger of a collection of sub-halo satellite systems having various masses. Dwarf spheroidal (dSph) systems observed today could be remaining evidence on the formation of the Galactic halo according to the hierarchical model (Menci et al., 2002). These dSphs have distinctly different environments than the Milky Way – notably their slow star formation rate and strong galactic winds that exhaust the gas content quickly (Lanfranchi & Matteucci, 2003). The low star formation rate, and thus slow metal enrichment, in dSph galaxies can result in a star carrying similar elemental abundances as a more metal-rich Galactic star. Hence, the α abundances in a dSph star could be relatively lower than the halo star at a given metallicity. The contribution of *s*-process nuclei, produced primarily in long-lived low to intermediate mass (LIM) stars, does not become important until [Fe/H]~ -1.0 dex in Milky Way. However, the *s*-process production may become significant at [Fe/H]~ -1.7 dex in dSph galaxies due to the slower metallicity increase (Venn et al., 2004; Lanfranchi et al.,

2008).

Furthermore, studies of presolar SiC grains show unexpected silicon isotopic ratios (see Zinner, 1998). Clayton (2003) suggests this puzzle can be solved if the solar birth environment was the remains of a merger event with a metal-poor satellite galaxy 5-6 Gyr ago. The stimulated star formation as a result of the merger gave rise to the asymptotic giant branch (AGB) stars that produce the observed solar Si isotopic ratios. A similar analysis on isotopic ratios of solar oxygen explains the high ^{18}O ratio as being due to the feedback of SNe outbreaks caused by the merger of a satellite galaxy with Milky Way (Clayton, 2004).

An alternative interpretation for why some metal-poor halo stars exhibit unexpected low [α/Fe] ratios could be due to the contamination of stellar surface by foreign material. A star may collect material from its ambient environment, thereby changing its surface chemical composition. Shigeyama & Tsujimoto (2003) explain the low [α/Fe] ratios of some Galactic halo stars being caused by them accreting dust grains or planetesimals. Mixing of the accreted material increases the surface Fe abundance relative to the α-elements (e.g. O), leading to a relatively low [α/Fe]. Smith et al. (2001) examine elemental abundances of a 1.23M$_\odot$ disk star (HD 19994) known to host a 2 M$_J$ planet orbiting with a semimajor axis of 1.3 AU. This particular star shows enrichment in its metal content with an overall overabundance of 0.13 dex relative to the Sun. Furthermore, their abundance analysis on various elements of planet host stars suggests the elemental abundances increase with condensation temperature (T$_c$) of the element. Volatile elements (low T$_c$) are less abundant, whereas refractory elements (high T$_c$) are relatively more abundant. In the circumstellar environment, refractory elements could condense closer to the star where the temperature is higher (forming terrestrial-like bodies). On the other hand, volatile elements would condense at lower temperatures i.e. farther away from the star (forming Jovian-like bodies). Planet host stars exhibiting higher abundances of refractory elements could suggest they accreted nearby refractory material, while Jovian (volatile-rich) bodies that form further out may maintain orbital stability. Thus, the relative abundance of volatile elements is less prominent

than the enhanced abundance of refractory elements.

Motivated by these diverse scenarios, we will investigate two metal-poor ([Fe/H]~ -1.50) halo stars HD 134439 and 134440 that show low [α/Fe] ratios (King, 1997a). These two main sequence dwarf stars are a weakly gravitationally bounded high proper motion pair that share a common history – i.e., similar age, kinematics, and chemical evolution. These observed properties suggest they were born in the same environment. HD 134439 and 134440's low [α/Fe] ratios could be the result of stellar accretion of circumstellar material, or this could suggest the stars might have a different origin than genuine Galactic halo stars. We seek to understand the physical mechanism that caused the low [α/Fe] nature for these stars by analyzing the abundances of various elements. In particular, we present abundances for the volatile elements carbon, nitrogen, oxygen, and some r-process elements. We investigate whether there exists a relationship between elemental abundances and condensation temperature, and explore the cause of the low [α/Fe] ratios in these stars. Our results could help better explain the role of low α metal-poor stars in the formation and evolution of galaxies.

A.2 DATA AND ANALYSIS

A.2.1 *Observations*

High-resolution (R=49,000) spectroscopy of HD 134439 and 134440 was obtained on UT 19 June 2006 using the HIRES spectrograph on the W.M. Keck I 10-m telescope (Table A.1). The useful wavelength coverage of the echelle spectra extends from 3020 Å to 5800 Å. Standard echelle reductions (debiasing, flat-fielding, order tracing and extraction, and wavelength calibration) were carried out. The per-pixel signal-to-noise ratio (S/N) is measured from Poisson statistics in the pseudo-continuum near the features. Certain regions of spectra overlapped in two adjacent orders and were coadded to increase S/N ratio. The final average S/N values near the CH, NH, and OH features of interest here are listed in Table A.1.

A.2.2 *Basic Physical Parameters*

Metallicity ([Fe/H]), surface temperature ($T_{\rm eff}$), and microturbulent velocity (ξ) of HD 134439 and 134440 listed in Table A.2 are obtained from King (1997a). The surface gravity, $\log g$, of HD 134439 and 134440 was taken from a 12 Gyr Yonsei-Yale (Y^2) isochrone (Demarque et al., 2004) with [α/Fe]=0, [Fe/H]= -1.50, and the Lejeune et al. (1998) color table. HD 134439 ($T_{\rm eff}$ = 5000 K) has a surface gravity of $\log g$ = 4.77 dex; HD 134440 ($T_{\rm eff}$ = 4785 K) has a corresponding value of $\log g$ = 4.79 dex. Alternatively, $\log g$ can be calculated according to the following,

$$\log \frac{g}{g_{\odot}} = \log \frac{\rm M}{\rm M_{\odot}} + 4 \log \frac{\rm T_{eff}}{\rm T_{eff,\odot}} + 0.4 {\rm V_{\circ}} + 0.4 BC + 2 \log \pi + 0.12 \qquad \text{(A.1)}$$

where M is the mass, $V_{\circ}$ is the apparent magnitude, π is the parallax in arcsec, and the bolometric correction (BC) is given by

$$BC = {\rm M}_{bol,\odot} - {\rm M_V} - 2.5 \log \frac{\rm L}{\rm L_{\odot}} \qquad \text{(A.2)}$$

we take $M_{bol,\odot}$=4.711 (from Lejeune et al. 1998 color table according to Yi et al. 2001), the Hipparcos-based M_V values from Table A.1, and $\log \frac{L}{L_{\odot}}$ is -0.8286 for HD 134439 and -0.9314 for HD 134440 from the Y^2 isochrone. Using equation A.1 with $\log g_{\odot}$=4.44 dex, $T_{\rm eff,\odot}$=5770 K, and values in Table A.1, we calculate $\log g$ of 4.61 dex and 4.63 dex for HD 134439 and 134440, respectively. Averaging $\log g$ values from isochrone and parallax calculation, we obtain 4.69 dex for HD 134439 and 4.71 dex for HD 134440, and suggest a plausible uncertainty at the $\pm$0.10 dex level.

A.2.3 *Abundance Analysis*

The new abundances presented here are determined from spectrum synthesis carried out in LTE with the MOOG package (Sneden, 1973) and LTE Kurucz model atmospheres corresponding to the parameters in Table A.2.

The line list used for the 3167.17 Å OH line is compiled by Schuler et al. (2006). Other line lists used in this study are compiled from Kurucz atomic and molecular lines (Kurucz, 1995), Vienna Atomic Line Database (Kupka et al., 2000), CH molecular lines from Jorgensen et al. (1996), and molecular lines simulated by LIFBASE (Luque & Crosley, 1999). CH, NH and OH diatomic dissociation energies adapted in the line lists are 3.47 eV, 3.45 eV and 4.39 eV, correspondingly. Oscillator strengths (gf-values) were adjusted to produce solar syntheses matching the Kurucz solar flux atlas (Kurucz, 2005). The synthetic solar spectra are generated with solar abundance of elements (except C, N, and O) built into MOOG from Anders & Grevesse (1989). The solar carbon and nitrogen abundances are from Asplund et al. (2005), while the solar oxygen abundance is from Allende Prieto et al. (2001). The desired stellar spectral regions are then synthesized using MOOG's synth driver with the model atmospheres and calibrated line lists.

The input elemental abundances in the syntheses are by default scaled to the Sun with [Fe/H] of -1.47 dex and -1.53 dex for HD 134439 and 134440, respectively. However, we have manually input the elemental abundances previously obtained for HD 134439 and 134440 in the literature (all but C, N, O, Fe, and Ag in Table A.7). The Gaussian smoothing factor for the syntheses is obtained from full-width-at-half-maximum measurements of various observed spectral lines that are clean and at comparatively redder wavelength (4000-5800 Å) than the lines used to measure the elemental abundances in this study.

The observed spectra for the stars were first normalized relative to the pseudo-continuum with SPECTRE (Fitzpatrick & Sneden, 1987). Wavelength shifts and flux rescaling of the observed spectra could be applied to improve the match with the synthetic spectra generated by MOOG. By comparing the synthesized spectra with the normalized observed spectra, we determine the abundances of the features by finding the best fit using χ^2-tests on regions centered around the features. We selected features that are strong and clean enough to allow good abundance measurements, and discarded those that are too saturated or blended.

After initial carbon, nitrogen and oxygen abundances were measured, they were

used as input for new syntheses in order to calibrate molecular equilibrium. Repeated iterations indicate minimal variations in C, N and O abundances. In fact, the only change recorded was a 0.01 dex decrease in carbon abundance for HD 134440. All other elemental abundances stay fixed within 0.01 dex. The abundances reported in Tables A.3, A.4, and A.5 are final measurements after achieving molecular equilibrium.

A.2.4 *Carbon Abundances*

A total of seven CH molecular lines were used in the $\lambda 4322 - 4326$ G-band region to measure the carbon abundance (see Figure A.1). The abundances are measured by applying χ^2-test to individual lines, instead of the entire band. Final best fit abundances of the lines are listed in Table A.3. The mean carbon abundances found for HD 134439 and 134440 are $\log N(\mathrm{C})_{39} = 6.49$ and $\log N(\mathrm{C})_{40} = 6.16$, respectively. The carbon to hydrogen ratios relative to the Sun are $[\mathrm{C/H}]_{39} = -1.90$ for HD 134439 and $[\mathrm{C/H}]_{40} = -2.23$ for HD 134440 assuming (self-consistently) the solar carbon abundance used in our line list calibration.

A.2.5 *Nitrogen Abundances*

Four NH molecular lines in the $\lambda 3326 - 3332$ region were used for the calculation of the nitrogen abundance (see Figure A.2 for partial synthesis). Although there are more than four NH features in the spectral region, we deemed them as too strong or blended for obtaining a good estimate of the nitrogen abundance. The abundances corresponding to the best fit between the synthetic and observed spectra for individual NH lines are listed in Table A.4. The resulting average nitrogen abundances are $\log N(\mathrm{N})_{39} = 5.83$ and $\log N(\mathrm{N})_{40} = 5.68$. The ratios compared to the Sun are $[\mathrm{N/H}]_{39} = -1.95$ and $[\mathrm{N/H}]_{40} = -2.10$.

A.2.6 *Oxygen Abundances*

The oxygen abundance is measured with seven near-UV electronic OH molecular lines in the spectral range $3129 - 3168$Å (e.g., Figure A.3). Results are listed in Table A.5. Final average oxygen abundances are $\log N(\mathrm{O})_{39} = 7.02$ and $\log N(\mathrm{O})_{40} = 6.83$. Oxygen to

hydrogen ratios relative to the Sun are $[O/H]_{39} = -1.67$ and $[O/H]_{40} = -1.86$.

The final carbon, nitrogen, and oxygen abundances are normalized with respect to the Sun. The results are independent of adopted gf-values and solar abundances for the line elements. Assuming solar abundances different from those employed in this study would require modifications of the gf-values in the line lists to re-match the solar atlas. Resulting stellar syntheses would produce elemental abundances that are adjusted accordingly. Hence, abundances of the elements when compared to the Sun will remain consistent regardless of the solar values assumed.

A.2.7 *Abundance Sensitivities and Uncertainties*

The abundances measured for HD 134439 and 134440 are sensitive to various quantities including surface temperature $\Delta T_{\rm eff}$, surface gravity $\Delta \log g$, microturbulent velocity $\Delta\xi$, uncertainty in setting pseudo-continuum $\Delta cont$, and statistical uncertainty σ. The sensitivities due to stellar atmospheric parameters are derived from syntheses by varying parameter values – i.e. $\pm$150 K for $T_{\rm eff}$, $\pm$0.20 dex for $\log g$, and $\pm$0.5 km/s for ξ. The sensitivity of [X/Fe] for each varied parameter is given by Δ[X/Fe] = Δ[X/H] $-$ Δ[Fe/H], where X could be C, N, or O. The sensitivities of [Fe/H], denoted by Δ[Fe/H], are taken from Table 3 of King (1997a). The results are listed in columns 2, 3 and 4 of Table A.6.

The elemental abundances could be uncertain due to (pseudo-)continuum setting. The continuum in the near-UV spectra is hard to determine, though the syntheses provide guidance. By altering the continuum settings by plausible amounts, we believe the 1 σ level uncertainties in the average abundance of C, N and O are about 0.04 dex to 0.06 dex.

The spread of abundances measured for each element from various molecular lines is 0.19 dex for C, 0.15 dex for N, and 0.34 dex for O. Therefore, it is important to analyze the statistical uncertainties in calculating mean abundances. The abundances of 7 CH lines, 4 NH lines and 7 OH lines in Tables A.3, A.4, and A.5 yield uncertainties of the mean: $\sigma_{\mu(\rm C)} = 0.07$ dex for [C/H], $\sigma_{\mu(\rm N)} = 0.04$ dex for [N/H], and $\sigma_{\mu(\rm O)} = 0.10$ dex for [O/H] averaged over HD 134439 and 134440. The uncertainty for the mean [Fe/H] value

is $\sigma_{\mu(\mathrm{Fe})} = 0.02$ dex (King, 1997a). Therefore, the statistical uncertainties, σ, for [C/Fe], [N/Fe] and [O/Fe] are propagated as $\sigma = \sqrt{\sigma^2_{\mu(\mathrm{X})} + \sigma^2_{\mu(\mathrm{Fe})}}$. The uncertainties for mean [X/Fe] are 0.07 dex, 0.05 dex and 0.10 dex for C, N and O correspondingly.

The final average uncertainty for HD 134439 and 134440 are found by adding the three parameter-based, continuum-based, and statistical uncertainties in quadrature. The [O/Fe] abundance is the most uncertain at $\pm$0.13 dex. Carbon and nitrogen uncertainties, both $\pm$0.09 dex, are slightly lower than oxygen. The major contribution of uncertainty originates from variations in T_{eff} (see Table A.6). Elemental abundances are less sensitive to other quantities, especially ξ.

A.3 RESULTS AND DISCUSSION

In Table A.7, we list relative element to iron ratios compared to the Sun, [X/Fe], for 22 elements. Carbon, nitrogen, oxygen, and silver abundances are those derived in this study, while [Fe/H] are from King (1997a) and 17 other elemental abundances are from Chen & Zhao (2006). Column 2 and 3 of Table A.7 list the [X/Fe] ratios for HD 134439 and 134440, respectively. Column 4 is the average [X/Fe] ratio and its uncertainties. The condensation temperatures for the elements are listed in column 5 (from Table 8 of Lodders, 2003).

A.3.1 *Abundances and T_{c}*

Figure A.4 shows the abundance results from Table A.7. The mean carbon, nitrogen, and oxygen abundances (at low T_{c}) for HD 134439 and 134440 are comparatively lower than the abundances of refractory elements at high T_{c}. The Spearman's rank coefficient (0.422) suggests a correlation between the elemental abundance and condensation temperature at the $\sim$5% significance level, perhaps reinforcing Shigeyama & Tsujimoto's (2003) hypothesis of planetesimal accretion from the circumstellar environment. The mean difference in abundance ratios from Table A.7 (HD 134439 $-$ HD 134440) is $-$0.02 dex with a scatter ($\pm$0.08 dex) consistent with uncertainties. Precise fine tuning must have

been required for them to now exhibit indistinguishable post-accretion abundance patterns given possible differences in circumstellar environments, stellar convection zone depths, and mass/composition of accreted material. Such a remarkable circumstance motivates us to revisit a nucleosynthetic examination of these stars' abundances.

A.3.2 *Comparisons with the Galactic Halo*

To begin reinvestigating the origin of HD 134439 and HD 134440, we compared their elemental abundances to stars of similar metallicity in the Galactic halo. We adopted typical [X/Fe] ratios of halo stars with [Fe/H]~ -1.50, mostly from observational data compiled by Kobayashi et al. (2006, see data sources referenced in the paper). The [Ag/Fe] ratio is for HD 103095 ([Fe/H]$= -1.31$) from Crawford et al. (1998). Other exceptions include abundance ratios for Al and K compiled by Timmes et al. (1995, and references therein), and for Y and Ba compiled by Travaglio et al. (2004a). We believe the high [N/Fe] ratio at [Fe/H]~ -1.50 in Kobayashi et al. (2006) is the result of mixing in evolved giants. The near-UV NH-based [N/Fe] values of unmixed or unevolved stars from the studies of Spite et al. (2005) and Israelian et al. (2004) consistently indicate that [N/Fe]=0.0 at [Fe/H]$= -1.5$. The flat behavior of [N/Fe] with [Fe/H] (long suspected despite grave uncertainties in the N abundances; e.g., Wheeler et al. 1989 and Prantzos 2003) and [N/Fe]=0.0 is also in excellent agreement with a metal-poor ([Fe/H]< -1) extension of the CN-based [N/Fe] ratios of the more-metal rich giants from Carretta et al. (2000) that are presumably immune from the effects of CN-cycling.

The mean abundance ratios of [Fe/H]~ -1.50 halo stars (Figure A.5: upper panel) have a negligible correlation with condensation temperature. The stark contrast with the mean ratios of HD 134439 and 134440 is shown in the lower panel of Figure A.5, which shows the differences (our stars $-$ halo) in [X/Fe] ratios versus T_c. The abundance differences demonstrate a correlation at less than 1% significance level. The results seem to imply a significant difference between the abundance patterns in HD 134439 and 134440 and typical halo filed stars.

However, some abundances do exhibit similarity with stars in the Galactic globular clusters. Considerable evidence for proton-capture nucleosynthesis has been observed in globular cluster giants in the halo (Kraft, 1994; Pilachowski et al., 1996; Kraft et al., 1997, 1998). Deep mixing in situ or in previous stellar generations having enriched the cluster gas has apparently enhanced cluster giant N, Na, and Al abundances by converting the C O, Ne, and Mg nuclei through proton-capture. As a result, one observes low [O/Fe] and [Mg/Al] ratios for many cluster giants compared to the typical enhancement of O and Mg observed in field halo giants and expected from Type II SNe nucleosynthesis.

The mean Galactic halo field data (Figure A.5) evince [O/Fe]$\sim$ 0.57 and [Mg/Al]$\sim$ 0.70 at [Fe/H]~ -1.50. The results in Table A.7 indicate HD 134439 and 134440 are ~ 0.85 dex lower in [O/Fe] and ~ 0.60 dex lower in [Mg/Al] compared to halo field stars, exhibiting underabundances of [O/Fe] and [Mg/Al] similar to many globular cluster giants. The Na and N abundances of HD 134439 and 134440, however, indicate this similarity is unrelated to proton-capture. Cluster giants with [O/Fe]~ -0.25 demonstrate [Na/Fe]$\sim$ 0.40 (see Figure 4 of Kraft et al. 1998). However, the mean [Na/Fe]~ -0.52 for HD 134439 and 134440 shows no evidence of such enhancement. In fact, the Na abundance is low compared to the mean halo field data (-0.16 dex). Similarly, our nitrogen abundance is also inconsistently lower than observed proton-capture processed material in cluster giants or in the mean halo field. Hence, we reject proton-processing as the agent responsible for our stars' anomalous abundances with respect to the halo field.

A.3.3 *Extragalactic Origins*

The low [α/Fe] and [Na/Fe] halo stars in Nissen & Schuster's (1997) study correspond to large apogalactocentric distance (R_{max}) and large maximum distance from galactic disk (z_{max}). They hypothesize an extragalactic origin (e.g., dwarf galaxies) for these anomalous stars. HD 134439 and 134440 also exhibit low [α/Fe] and [Na/Fe] with large R_{max} ($\sim$ 43 kpc). Based on the kinematics and abundances of these stars, Chen & Zhao (2006) posit a dSph galaxy origin for them. In addition, they suggest formation in a high

dust-to-gas environment to explain the gross correlation of abundances with condensation temperature and particular patterns in the α elements. This hypothesis provides an alternative to Shigeyama & Tsujimoto's (2003) planetesimal accretion mechanism to explain the abundance trend with T_c.

We show stellar abundances for giants in dSph galaxies gathered from literature sources in Figures A.6 and A.7. The abundances for Sagittarius (Sgr) are obtained from Bonifacio et al. (2000, 2004), Monaco et al. (2005), and Smecker-Hane & Mc William (1999). We use the Shetrone et al. (2001, 2003) studies for giants in Draco (Dra), Ursa Minor (UMi), Sextans (Sex), Sculptor (Scl), Fornax (For), Carina (Car), and Leo I. We have also adopted Geisler et al.'s (2005) abundance measurements for four red giants in Scl. The collection of studies cover the metallicity range of $-3 \lesssim$[Fe/H]$\lesssim 0$. The top panel of Figure A.8 shows mean [X/Fe] ratios for dSph giants at [Fe/H]~ -1.50 from the data collected in Figures A.6 and A.7. The differences from mean HD 134439 and 134440 ratios are shown in the lower panel of Figure A.8. A Spearman's rank correlation test reveals no significant correlation between the HD 134439/440 − dSph abundance differences and T_c. This suggests that dust may not have played any greater role in the formation of HD 134439 and 134440 compared to in situ dSph stars.

This lack of a clear correlation of differences in our stars' abundances and those of dSph systems with T_c motivated us to consider a pure nucleosynthetic explanation of the abundances whose correlation with T_c, if any, might simply be illusory. Tolstoy et al. (2003) analyze stellar abundances in four dSph galaxies and find their results to lack any evidence of explosive nucleosynthesis from stars with progenitor mass $\geq 15 - 20$ $M_\odot$. We explore the same possibility here using the Type II yields of Kobayashi et al. (2006), and find that explosive nucleosynthesis in Type II SNe of low progenitor mass provides a consistent and unique explanation for the majority of abundance patterns in HD 134439 and 134440.

Figures A.5 and A.8 show that the [O/Fe] ratio of our two stars is, like the α elements of higher T_c, low compared to Galactic halo and other dSph's. While, moreover, our [O/Fe] ratio is $\sim$0.35 dex lower than ratios of other α elements in our stars (Figure A.4),

this may have little to do with T_c-related behavior. The [O/Fe] yields in the Z=0 Type II models of Kobayashi et al. (2006) are steep functions of mass – e.g., being some 0.60 dex lower for progenitors of 14 $M_\odot$ than for 20 $M_\odot$. In contrast, the [Mg/Fe] and [Si/Fe] yields are much shallower functions of mass, with yields changing by ≤ 0.20 dex over the same progenitor mass range. Formation from material enriched by Type II SNe biased towards low progenitor mass is qualitatively consistent with the markedly low [O/Fe] ratio in our stars. Indeed, for progenitor mass of 14 $M_\odot$, the [Mg/Fe] and [Si/Fe] yields are some 0.30 dex larger than for [O/Fe], a difference in excellent agreement with our abundance results. The [C/Fe] and [N/Fe] ratios of our stars are also low compared to the Galactic halo (Figure A.5), and a factor of two even lower than the [O/Fe] ratio (Figure A.4). However, this too need have little to do with T_c-related effects. Chemical evolution models of dSph galaxies predict [N/O] and [C/O] ratios as low as -1 dex (Figure 13 of Carigi & Hernandez 2008), easily accommodating the values of ~ -0.30 in our stars.

The Galactic potassium abundance data used in Figure A.5 exhibit behavior strongly reminiscent of traditional α-elements. Thus, one need not make recourse to T_c-related effects to explain the abnormally low [K/Fe] ratio of our stars compared to Galactic halo (the same behavior exhibited by the α elements). The Kobayashi et al. (2006) [Na/Fe] yields also drop precipitously over the 20 to 14 $M_\odot$ progenitor mass range like those for [O/Fe]. The [Na/Fe] ratio of our stars is well matched by the Kobayashi et al. (2006) yields at 14 $M_\odot$; its distinctly sub-solar value (~ -0.50) is thus easily explained without recourse to T_c-related effects.

The low [Cu/Fe] ratio (~ -0.70 for HD 134439 and 134440) also need not be associated with T_c-related effects since it is not significantly different than the ratio observed in Galactic halo stars or dSph stars (Figures A.5 and A.8). As noted by Timmes et al. (1995), Galactic halo Cu data are consistent with the Type II yields of Woosley & Weaver (1995) that suggest Cu production in the halo is dominated by explosive nucleosynthesis and not production in Type Ia supernovae or LIM stars. The [Zn, Ni, Co/Fe] ratios of our stars are all in outstanding agreement with the Kobayashi et al. yields (which rise steeply with

decreasing progenitor mass for these 3 elements) at a progenitor mass of 14 $M_{\odot}$. Our [Al, Cr/Fe] ratios are also nearly identical to the Kobayashi et al. yields for a 14 $M_{\odot}$ progenitor.

A couple possible puzzles remain worthy of comment. As pointed out by Venn et al. (2004), dSph [Ti,Ca/Fe] ratios appear to be lower than [Mg/Fe] ratios; this result is in good accord with the Kobayashi et al. (2006) [X/Fe] yields at low progenitor mass. However, as already noted by Chen & Zhao (2006), our stars' [Ti,Ca/Fe] ratios are both larger than the [Mg/Fe] ratio. Second, the observed [Mn/Fe] ratio is 0.30 dex larger than the Kobayashi et al. (2006) [Mn/Fe] yield at 14 $M_{\odot}$. However, our stars do not appear to be anomalous with respect to dSph objects; Figure A.8 indicates that dSph [Mn/Fe] ratios at [Fe/H]$= -1.50$ are identical to those in HD 134439 and HD 134440.

The abundance ratios excluding [Ca,Ti/Fe] provide strong support for a nucleosynthetic explanation of the HD 134439/440 abundance patterns that are dominated by low mass progenitor Type II SNe products, and correlations with T_c being simply illusory. We find no observable evidence of Type Ia contributions consistent with the observed abundance data. Such contributions are of possible interest in explaining the overall values of [O/Fe] and [Mn/Fe] ratios, which are some 0.30 dex lower and higher (respectively) than the Kobayashi et al. (2006) 14 $M_{\odot}$ progenitor yields; these differences are qualitatively consistent with lower and higher (respectively) Type Ia yields for these two ratios.

We made simple Type II/Ia mixture models from the Kobayashi et al. (2006) Type II yields for a range of progenitor masses and weighted Type Ia yields from Thielemann et al. (2003) as tabulated in Travaglio et al. (2004b); the Type Ia weighting factors were those producing the observed mean [O/Fe] ratio of our stars. Resulting [X/Fe] yields from the mixtures were computed for elements other than O. We find that such mixtures are unsatisfactory in explaining the observed abundance ratios. For example, simultaneously the [Ni/Fe] yields are ≥ 0.30 dex larger than observed, [Mn/Fe] becomes overenhanced by ≥ 0.25 dex, [Na/Fe] is ≥ 0.30 lower than observed, and the predicted [Ti/Fe] yields become even lower compared to the data.

A.3.4 *Neutron-capture Elements*

As noted by Chen & Zhao (2006), HD 134439 and 134440 exhibit a peculiar n-capture abundance pattern. The mean [Ba/Y]~ -0.10 is smaller (though perhaps not significantly) than the +0.20 exhibited by Galactic halo stars of similar metallicity (see Figure A.5), and markedly lower than typical values of +0.60 evinced by dSph stars (Shetrone et al., 2003; Venn et al., 2004). At [Fe/H]~ -1.50, Ba is produced via the r-process while Y is produced via the r-process and the putative light element primary process (LEPP; Travaglio et al., 2004a). The mean dSph ratio [Ba/Y]$\sim +0.60$ is in excellent agreement with the r-process ratio predicted by Galactic chemical evolution models as seen in Figure 12 of Travaglio et al. (2004a), who speculated the large pure r-process-like ratio might be driven by a deficiency in Y caused by loss of LEPP-rich ejecta to the ISM in dSph systems.

Our near solar [Ba/Y] ratio, similar to that seen in the Galaxy, then might be explained if the ISM of the parent dSph that birthed HD 134439 and 134440 was simply able to retain Y-rich LEPP products. However, we believe this is not the whole story. The mean [Y/Fe] ratio of our two stars only differs by 0.1-0.2 dex with respect to either the mean Galaxy or dSph ratios at [Fe/H]~ -1.50, while [Ba/Fe] differs by 0.4-0.5 dex; it is thus Ba, and not Y, that is the anomaly in our stars' unexpected [Ba/Y] ratio. In order to test this conclusion, we need to examine other abundances with a likely pure r-process origin. We selected the canonical r-process tracers Eu along with Ag. Silver may seem to be an unconventional choice. However, its great utility comes from observably strong transitions of *neutral* features in the near-UV; the observed n-capture transitions upon which most of our knowledge of Galactic and dSph abundance patterns are built (via observation in low gravity red giants) are singly ionized lines; however, these become vanishingly weak in our metal-poor cool dwarfs. The limited halo data (Crawford et al., 1998) suggest an r-process origin of Ag in metal-poor Galactic stars.

The [Ag/Fe] ratios for HD 134439 and HD 134440 are measured from the λ3280 and λ3382 Ag I lines. Line lists are compiled for the Ag line regions using VALD and

assuming a solar Ag abundance of $\log N(\mathrm{Ag})_{\odot} = 1.54$. Synthesizing the spectra with MOOG yields [Ag/Fe]= -0.19 dex for HD 134439 (Figure A.9) and -0.13 dex for HD 134440. Crawford et al. (1998) studied the [Ag/Fe] ratios of the metal-poor halo dwarf HD 103095, which has physical properties (T_{eff}, [Fe/H], $\log g$) similar to HD 134439. They obtained a mean [Ag/Fe] ratio of +0.28 dex for HD 103095 by measuring the same Ag I lines. The underabundance of silver compared to HD 103095 can easily be seen by comparing the relative strengths of the neighboring Ag I and Fe I lines in Figure A.9 to Figure 3 of Crawford et al. (1998).

The europium abundances are estimated by synthesizing the λ4205 Eu II lines for HD 134439, 134440, and 103095 (using a high S/N R$\sim$60,000 spectrum obtained with the McDonald Observatory 2.7m 2dCoude spectrograph). A Kurucz LTE model atmosphere for HD 103095 is generated with the physical parameters described in King (1997b): $T_{\mathrm{eff}} = 5050$ K, [Fe/H]= -1.31, $\log g = 4.5$, and $\xi = 1.5$ km/s. The line profile at 4205.04Å appears blended in our stars and we encountered difficulties simultaneously and consistently fitting the wings of line in the stars and the Sun (for which we assumed $\log N(\mathrm{Eu})_{\odot} = 0.51$ in making gf-value adjustments). We believe it is safe only to establish upper limits on [Eu/Fe] by fitting the line bottom at 4205.04Å, giving ratios of $\lesssim +0.31$ dex for HD 134439, $\lesssim +0.42$ dex for HD 134440, and $\lesssim +0.70$ dex for HD 103095. The suggestion that [Eu/Fe] is $\sim 0.30 - 0.40$ dex larger in HD 103095 is confirmed in Figure A.10, where we compare the observed spectra of HD 103095 (dotted line) with HD 134439 (solid line). Four spectral regions are shown to confirm the consistent observations of stronger europium relative to other metal features in HD 103095.

We conclude that the [Ba, Ag, Eu/Fe] ratios are consistently lower in HD 134439 and 134440 by about ~ 0.40 dex when compared to the halo star HD 103095. Our results suggest that HD 134439 and 134440 are deficient in heavy r-process products relative to light r-process products.

Figures 5 and 10 of Travaglio et al. (2004a) indicate that s-contributions from AGB stars alone would result in [Ba/Y]= +0.60 - +0.70 at [Fe/H]= -1.50 in the Galaxy. Indeed,

Venn et al. (2004) invoke such contributions to explain the large supersolar [Ba/Y] ratios in dSph stars; they do not explain our subsolar ratio. Qian & Wasserburg's (2001) schematic Galactic *r*-process model divides Type II SN into two classes– H and L. The L class Type II are less frequent events from lower mass stars that produce exclusively lighter (up to Ba) *n*-capture elements; H events are responsible for the production of heavier (A$\geq$ 130) *n*-capture elements, but produce light *n*-capture elements as well. Their phenomenal approach fits the Galactic *n*-capture abundance data well over the range $-3 \leq$ [Fe/H] ≤ -1 assuming no *s*-process contribution. The relative L-event yields in their Figure 2 produce the Ba/Ag and Ba/Y logarithmic number abundance ratios observed in our stars to within 0.17 dex. In contrast, their Figure 2 predicts Ba/Y ratios from H events some 0.80 dex larger than observed in our stars. The agreement of the light *n*-capture abundance ratios with the L-event yields is consistent with our previous conclusion that abundances in our stars are dominated by nucleosynthetic products from lower mass Type II events; our upper limit on Eu seems further consistent with this notion. Additional interpretation of the *n*-capture abundances in our stars in the framework of the L,H-event model schema will require measurements of possibly absent or highly underabundant additional heavy *n*-capture elements in our stars and computational exploration of possible L-event overflow that might allow the *r*-process to reach beyond A$\geq$ 130 and explain the detection of any such elements.

A final possible explanation of the *n*-capture ratios in our stars that might also account for the unexpectedly high [Ca,Ti/Fe] ratios is the α-process in a high neutron excess environment originally envisioned by Hoyle & Fowler (1960) and explored in detail by Woosley & Hoffman (1992); the latter show that, with sufficiently high neutron excess, the familiar α-rich freeze-out "merges" into what may be an (or *the*) *r*-process. This process provides a natural mechanism to overproduce both Ca and Ti relative to the other α-elements, consistent with the abundances in our two stars. Moreover, the production factors calculated under two different assumptions for model zone integration in Figure 2 of Woosley & Hoffman (1992) give [Ag/Y] ratios that bracket the observed ratio of our stars. While nucleosynthesis in such a high-entropy environment is a promising explanation for

the curious Ca, Ti, and n-capture abundances in our stars, a rigorous examination of this hypothesis requires abundance determinations of additional n-capture elements in our stars and calculations extended to atomic mass beyond Ag.

A.4 SUMMARY

Abundances of carbon, nitrogen, and oxygen are measured from the Keck high-resolution spectra for the metal-poor common proper motion pair HD 134439 and HD 134440. We obtain mean abundances [C/Fe]= -0.56, [N/Fe]= -0.52, and [O/Fe]= -0.26 for these two stars. An analysis of 22 elements demonstrates a strong correlation (at $\sim$5% significance level) between abundances and condensation temperature. Furthermore, a comparison of abundances in our stars to those in typical halo stars at similar metallicity demonstrates a significant correlation ($< 1\%$) for the abundance differences with T_c – suggesting HD 134439 and 134440 were born in an environment that is remarkably different from (e.g., dustier than) the Galactic halo. However, the abundance difference-T_c correlation is not significant ($> 30\%$) for stars in the dSph galaxies – i.e. the formation site of our stars is no dustier than typical star formation regions in dSphs.

On the other hand, this abundance behavior with T_c could be an illusory trend – perhaps accounted for by nucleosynthesis alone. Our analysis on individual elements indicates consistency with the production from Type II SNe of low mass progenitors. In fact, the yields of a $\sim 14 M_\odot$ Type II SNe progenitor (as described in Kobayashi et al. 2006) were able to match most of the observed abundances for HD 134439 and HD 134440 (exceptions include Ca and Ti). Attempts to explain the overabundances of Ca and Ti with addition of Type Ia yields only aggravate the problem.

In addition, the interesting abundance of [Ba/Y]~ -0.10 motivated our study of neutron-capture elements. We estimate a mean [Ag/Fe]= -0.16 and obtain an upper limit of $+0.37$ dex for [Eu/Fe]. This demonstrates the consistently low abundance (by ~ 0.40 dex) of r-process elements in HD 134439 and 134440 compared to typical halo stars. We consider Qian & Wasserburg's (2001) L class Type II SNe that produce mainly light n-

elements, as well as an α-rich freeze-out environment, as possible chemical origins for the n-elements observed in HD 134439 and HD 134440. However, further investigation on n-capture elements is needed to constrain their origin.

This work was supported by NSF grant AST 02-39518 to J.R.K.

Facilities: KECK

REFERENCES

Allende Prieto, C., Lambert, D. L., & Asplund, M. 2001, ApJ, 556, L63

Anders, E., & Grevesse, N. 1989, Geochim. Cosmochim. Acta, 53, 197

Asplund, M., Grevesse, N., & Sauval, A. J. 2005, Cosmic Abundances as Records of Stellar Evolution and Nucleosynthesis, 336, 25

Bonifacio, P., Hill, V., Molaro, P., Pasquini, L., Di Marcantonio, P., & Santin, P. 2000, A&A, 359, 663

Bonifacio, P., Sbordone, L., Marconi, G., Pasquini, L., & Hill, V. 2004, A&A, 414, 503

Brown, J. A., Wallerstein, G., & Zucker, D. 1997, AJ, 114, 180

Carigi, L., & Hernandez, X. 2008, ArXiv e-prints, 802, arXiv:0802.1203

Carney, B. W., Latham, D. W., Laird, J. B., & Aguilar, L. A. 1994, AJ, 107, 2240

Carney, B. W., Wright, J. S., Sneden, C., Laird, J. B., Aguilar, L. A., & Latham, D. W. 1997, AJ, 114, 363

Carretta, E., Gratton, R. G., & Sneden, C. 2000, A&A, 356, 238

Chen, Y. Q., & Zhao, G. 2006, MNRAS, 370, 2091

Clayton, D. D. 2003, ApJ, 598, 313

Clayton, D. D. 2004, Lunar and Planetary Institute Conference Abstracts, 35, 1045

Crawford, J. L., Sneden, C., King, J. R., Boesgaard, A. M., & Deliyannis, C. P. 1998, AJ, 116, 2489

Demarque, P., Woo, J.-H., Kim, Y.-C., & Yi, S. K. 2004, ApJS, 155, 667

Eggen, O. J., Lynden-Bell, D., & Sandage, A. R. 1962, ApJ, 136, 748

Fitzpatrick, M. J., & Sneden, C. 1987, BAAS, 19, 1129

Geisler, D., Smith, V. V., Wallerstein, G., Gonzalez, G., & Charbonnel, C. 2005, AJ, 129, 1428

Hoyle, F., & Fowler, W. A. 1960, ApJ, 132, 565

Israelian, G., Ecuvillon, A., Rebolo, R., García-López, R., Bonifacio, P., & Molaro, P. 2004, A&A, 421, 649

Jorgensen, U. G., Larsson, M., Iwamae, A., & Yu, B. 1996, A&A, 315, 204

King, J. R. 1997, AJ, 113, 2302

King, J. R. 1997, PASP, 109, 776

Kobayashi, C., Umeda, H., Nomoto, K., Tominaga, N., & Ohkubo, T. 2006, ApJ, 653, 1145

Kraft, R. P. 1994, PASP, 106, 553

Kraft, R. P., Sneden, C., Smith, G. H., Shetrone, M. D., Langer, G. E., & Pilachowski, C. A. 1997, AJ, 113, 279

Kraft, R. P., Sneden, C., Smith, G. H., Shetrone, M. D., & Fulbright, J. 1998, AJ, 115, 1500

Kupka, F. G., Ryabchikova, T. A., Piskunov, N. E., Stempels, H. C., & Weiss, W. W. 2000, Baltic Astronomy, 9, 590

Kurucz, R. L. 1995, Astrophysical Applications of Powerful New Databases, 78, 205

Kurucz, R. L. 2005, Memorie della Societa Astronomica Italiana Supplement, 8, 189

Lanfranchi, G. A., & Matteucci, F. 2003, MNRAS, 345, 71

Lanfranchi, G. A., Matteucci, F., & Cescutti, G. 2008, A&A, 481, 635

Lejeune, T., Cuisinier, F., & Buser, R. 1998, A&AS, 130, 65

Lodders, K. 2003, ApJ, 591, 1220

Luque, J., & Crosley, D. R. 1999, LIFBASE: Database and spectral simulation (version 1.5), SRI International Report MP 99-009

Menci, N., Cavaliere, A., Fontana, A., Giallongo, E., & Poli, F. 2002, ApJ, 575, 18

Monaco, L., Bellazzini, M., Bonifacio, P., Ferraro, F. R., Marconi, G., Pancino, E., Sbordone, L., & Zaggia, S. 2005, A&A, 441, 141

Nissen, P. E., & Schuster, W. J. 1997, A&A, 326, 751

Perryman, M. A. C., et al. 1997, A&A, 323, L49

Pilachowski, C. A., Sneden, C., Kraft, R. P., & Langer, G. E. 1996, AJ, 112, 545

Prantzos, N. 2003, Astronomical Society of the Pacific Conference Series, 304, 361

Prantzos, N. 2007, EAS Publications Series, 24, 3

Preston, G. W., & Sneden, C. 2000, AJ, 120, 1014

Qian, Y.-Z., & Wasserburg, G. J. 2001, ApJ, 559, 925

Schuler, S. C., Hatzes, A. P., King, J. R., Kürster, M., & The, L.-S. 2006, AJ, 131, 1057

Searle, L., & Zinn, R. 1978, ApJ, 225, 357

Shetrone, M. D., Côté, P., & Sargent, W. L. W. 2001, ApJ, 548, 592

Shetrone, M., Venn, K. A., Tolstoy, E., Primas, F., Hill, V., & Kaufer, A. 2003, AJ, 125, 684

Shigeyama, T., & Tsujimoto, T. 2003, ApJ, 598, L47

Smecker-Hane, T., & Mc William, A. 1999, Spectrophotometric Dating of Stars and Galaxies, 192, 150

Smith, V. V., Cunha, K., & Lazzaro, D. 2001, AJ, 121, 3207

Sneden, C. 1973, ApJ, 184, 839

Spite, M., et al. 2005, A&A, 430, 655

Thielemann, F.-K., et al. 2003, Nuclear Physics A, 718, 139

Timmes, F. X., Woosley, S. E., & Weaver, T. A. 1995, ApJS, 98, 617

Tolstoy, E., Venn, K. A., Shetrone, M., Primas, F., Hill, V., Kaufer, A., & Szeifert, T. 2003, AJ, 125, 707

Travaglio, C., Gallino, R., Arnone, E., Cowan, J., Jordan, F., & Sneden, C. 2004, ApJ, 601, 864

Travaglio, C., Hillebrandt, W., Reinecke, M., & Thielemann, F.-K. 2004, A&A, 425, 1029

Venn, K. A., Irwin, M., Shetrone, M. D., Tout, C. A., Hill, V., & Tolstoy, E. 2004, AJ, 128, 1177

Wheeler, J. C., Sneden, C., & Truran, J. W., Jr. 1989, ARA&A, 27, 279

Woosley, S. E., & Hoffman, R. D. 1992, ApJ, 395, 202

Woosley, S. E., & Weaver, T. A. 1995, ApJS, 101, 181

Yi, S., Demarque, P., Kim, Y.-C., Lee, Y.-W., Ree, C. H., Lejeune, T., & Barnes, S. 2001, ApJS, 136, 417

Zinner, E. 1998, Annual Review of Earth and Planetary Sciences, 26, 147

Table A.1. Observational Data

	HD 134439	HD 134440
RA (2000)	15:10:13.09	15:10:12.97
Dec (2000)	-16:22:45.85	-16:27:46.52
V	9.07	9.44
B-V	0.77	0.85
Date (MJD)	53905.314698	53905.325741
Exposure (s)	900	900
S/N (CH)	192	173
S/N (NH)	83	68
S/N (OH)	87	70
π[a](mas)	34.14	33.68
M[b]($M_\odot$)	0.57	0.54
M_V	7.076	7.392
U[b](km/s)	-310	-311
V[b](km/s)	-467	-473
W[b](km/s)	-44	-48

[a]From Perryman et al. (1997)

[b]From Table 6 of Carney et al. (1994)

Table A.2. Stellar Parameters

Parameters	HD 134439	HD 134440
[Fe/H][a](dex)	-1.47 ± 0.07	-1.53 ± 0.09
T_{eff}[a](K)	5000 ± 50	4785 ± 50
$\log g$ (dex)	4.69 ± 0.10	4.71 ± 0.10
ξ[a](km/s)	1.5 ± 0.3	1.5 ± 0.3

[a]Values from King (1997a).

Table A.3. Carbon Abundances

	HD 134439		HD 134440	
λ	$\log N(\mathrm{C})$	[C/H][a]	$\log N(\mathrm{C})$	[C/H][a]
Å	dex	dex	dex	dex
4323.02	6.52	-1.87	6.20	-2.19
4323.22	6.53	-1.86	6.21	-2.18
4323.50	6.55	-1.84	6.24	-2.15
4323.85	6.47	-1.92	6.09	-2.30
4324.12	6.52	-1.87	6.22	-2.17
4324.40	6.46	-1.93	6.11	-2.28
4324.81	6.36	-2.03	6.09	-2.30

[a]Assumed solar carbon abundance of $\log N(\mathrm{C})_{\odot} = 8.39 \pm 0.05$ dex (Asplund et al., 2005).

Table A.4. Nitrogen Abundances

	HD 134439		HD 134440	
λ	$\log N$(N)	[N/H][a]	$\log N$(N)	[N/H][a]
Å	dex	dex	dex	dex
3326.41	5.84	-1.94	5.76	-2.02
3328.20	5.84	-1.94	5.65	-2.13
3330.27	5.79	-1.99	5.61	-2.17
3330.92	5.83	-1.95	5.70	-2.08

[a]Assumed solar nitrogen abundance of $\log N(\mathrm{N})_{\odot} = 7.78 \pm 0.06$ dex (Asplund et al., 2005).

Table A.5. Oxygen Abundances

	HD 134439		HD 134440	
λ	$\log N(\mathrm{O})$	$[\mathrm{O/H}]^{a}$	$\log N(\mathrm{O})$	$[\mathrm{O/H}]^{a}$
Å	dex	dex	dex	dex
3129.94	7.11	-1.58	6.98	-1.71
3138.78	6.99	-1.70	6.76	-1.93
3138.92	6.93	-1.76	6.64	-2.05
3139.30	7.07	-1.62	6.73	-1.96
3140.51	7.06	-1.63	6.95	-1.74
3141.66	6.96	-1.73	6.93	-1.76
3167.17	7.03	-1.66	6.79	-1.90

[a]Assumed solar oxygen abundance of $\log N(\mathrm{O})_{\odot} = 8.69 \pm 0.05$ dex (Allende Prieto et al., 2001).

Table A.6. Abundance Sensitivities

	ΔT_{eff} ±150 K	$\Delta \log g$ ±0.20 dex	$\Delta\xi$ ±0.5 km/s	$\Delta cont$[a] dex	σ[b] dex	σ_{avg}[c] dex
Δ[C/Fe]	±0.09	∓0.04	±0.03	0.04	0.07	0.09
Δ[N/Fe]	±0.12	∓0.05	±0.02	0.06	0.05	0.09
Δ[O/Fe]	±0.15	∓0.06	±0.00	0.06	0.10	0.13

[a]This is the true uncertainty in setting the pseudo-continuum of the spectra.

[b]σ is the statistical uncertainty in calculating the mean abundance from the molecular lines measured.

[c]This is the average abundance uncertainty of HD 134439 and HD 134440 for the average [X/Fe] ratios.

Note. — We have adapted the sensitivities of [Fe/H] due to T_{eff}, $\log g$, ξ, and statistical uncertainty from Table 3 of King (1997a) for the calculations in this table.

Table A.7. Elemental Abundances

		HD 134439	HD 134440		
	X	[X/Fe]	[X/Fe]	$[X/Fe]_{avg}$ [a]	T_c [b]
		dex	dex	dex	K
	C	-0.43	-0.70	-0.56 ± 0.09	40
	N	-0.48	-0.57	-0.52 ± 0.09	123
	O	-0.20	-0.33	-0.26 ± 0.13	180
α	Mg	-0.09	-0.10	-0.10 ± 0.05	1336
elements	Si	+0.04	+0.04	+0.04 ± 0.10	1310
	Ca	+0.09	+0.08	+0.08 ± 0.04	1517
	Ti	+0.18	+0.20	+0.19 ± 0.09	1582
	Na	-0.48	-0.49	-0.48 ± 0.06	958
	Al	-0.22	-0.19	-0.20 ± 0.04	1653
	K	+0.10	+0.08	+0.09 ± 0.08	1006
odd Z	Sc	-0.03	-0.04	-0.04 ± 0.07	1659
elements	V	+0.01	+0.05	+0.03 ± 0.08	1429
	Mn	-0.41	-0.37	-0.39 ± 0.05	1158
	Co	-0.03	+0.05	+0.01 ± 0.05	1352
	Cu	-0.69	···	···	1037
	Fe [c]	(-1.47)	(-1.53)	(-1.50 ± 0.09)	1334
even Z	Cr	-0.01	+0.06	+0.02 ± 0.06	1296
elements	Ni	-0.12	-0.13	-0.12 ± 0.05	1353
	Zn	-0.04	-0.06	-0.05 ± 0.10	726

Table A.7 (cont'd)

n-capture	Y	-0.22	-0.28	-0.25 ± 0.08	1659
elements	Ag	-0.19	-0.13	-0.16	996
	Ba	-0.35	-0.36	-0.36 ± 0.07	1455

[a][X/Fe]$_{avg}$ is the average [X/Fe] ratios of HD 134439 and HD 134440.

[b]Condensation temperatures are taken from Table 8 of Lodders (2003).

[c]These are [Fe/H] values from King (1997a).

Note. — Elemental abundances and uncertainties, with the exception of C, N, O, Fe and Ag are taken from Table 1 of Chen & Zhao (2006).

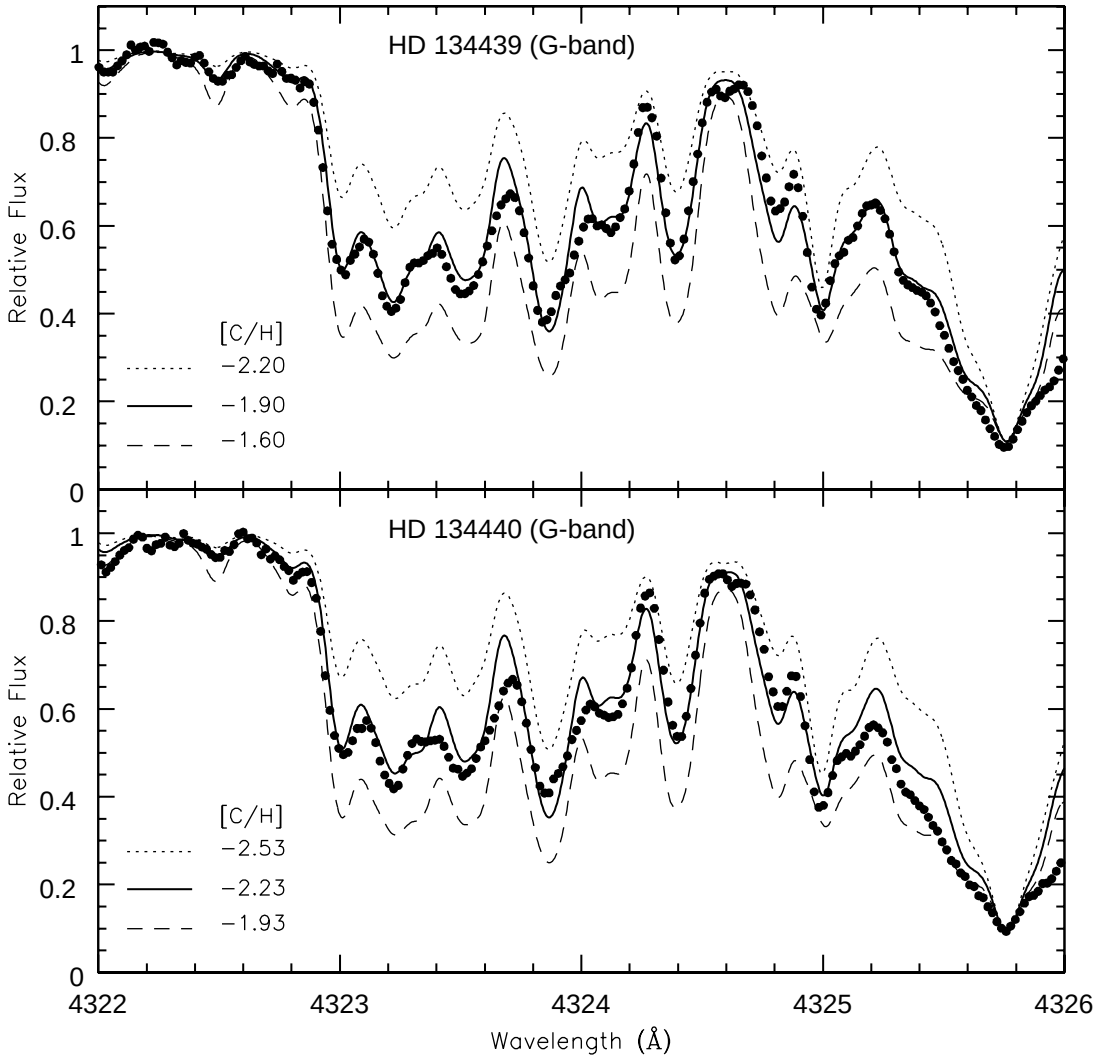

Figure A.1 G-band synthesis for HD 134439 (upper panel) and HD 134440 (lower panel). Filled circles indicate observed spectra. The solid line is the average best-fit [C/H] abundance by χ^2-tests on individual lines. Dotted and dashed lines are ±0.30 dex deviations from the best-fit abundance.

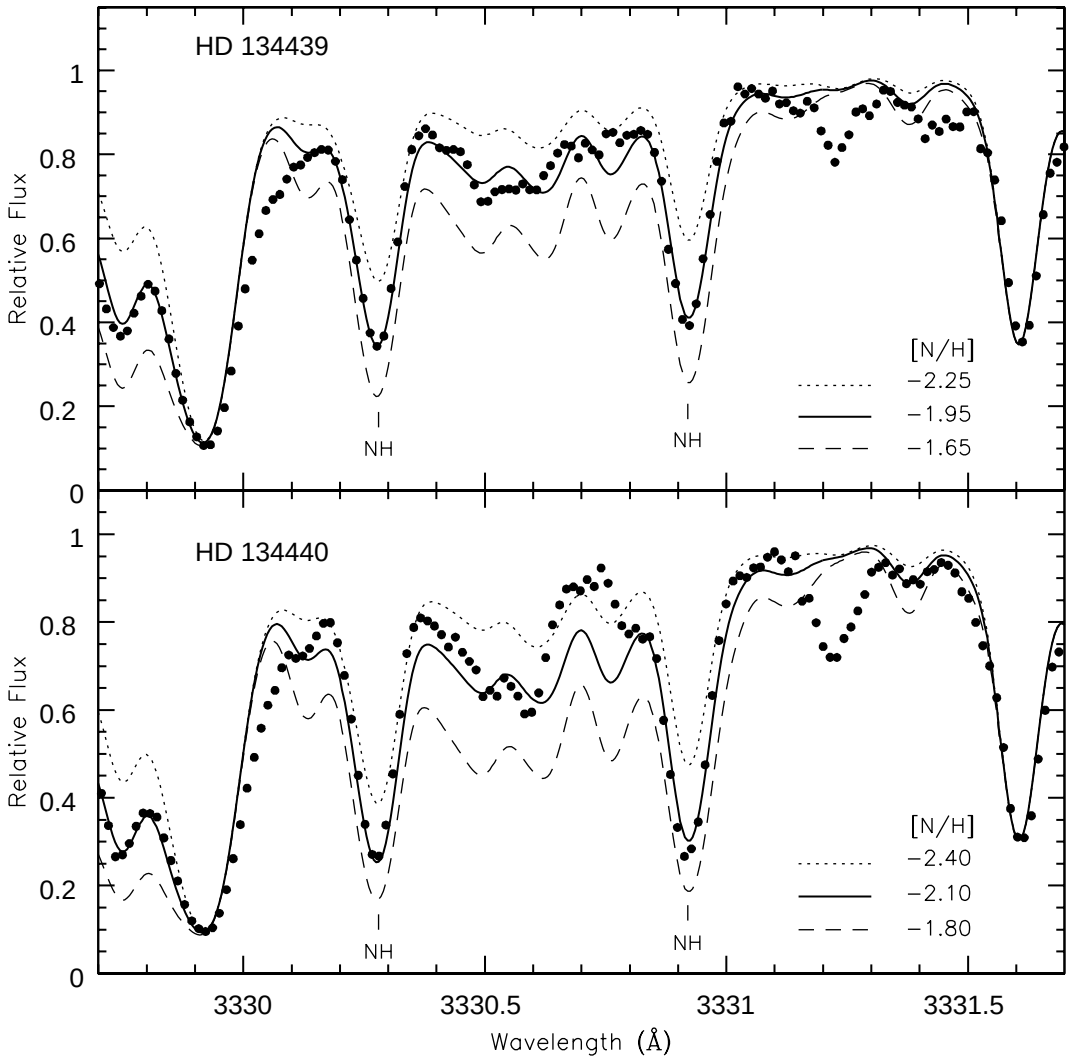

Figure A.2 Synthesis of NH molecular lines for HD 134439 (upper panel) and HD 134440 (lower panel). Filled circles indicate observed spectra. The solid line is the average best-fit [N/H] abundance by χ^2-test on the individual NH lines indicated. Dotted and dashed lines are ± 0.30 dex deviations from the best-fit abundance.

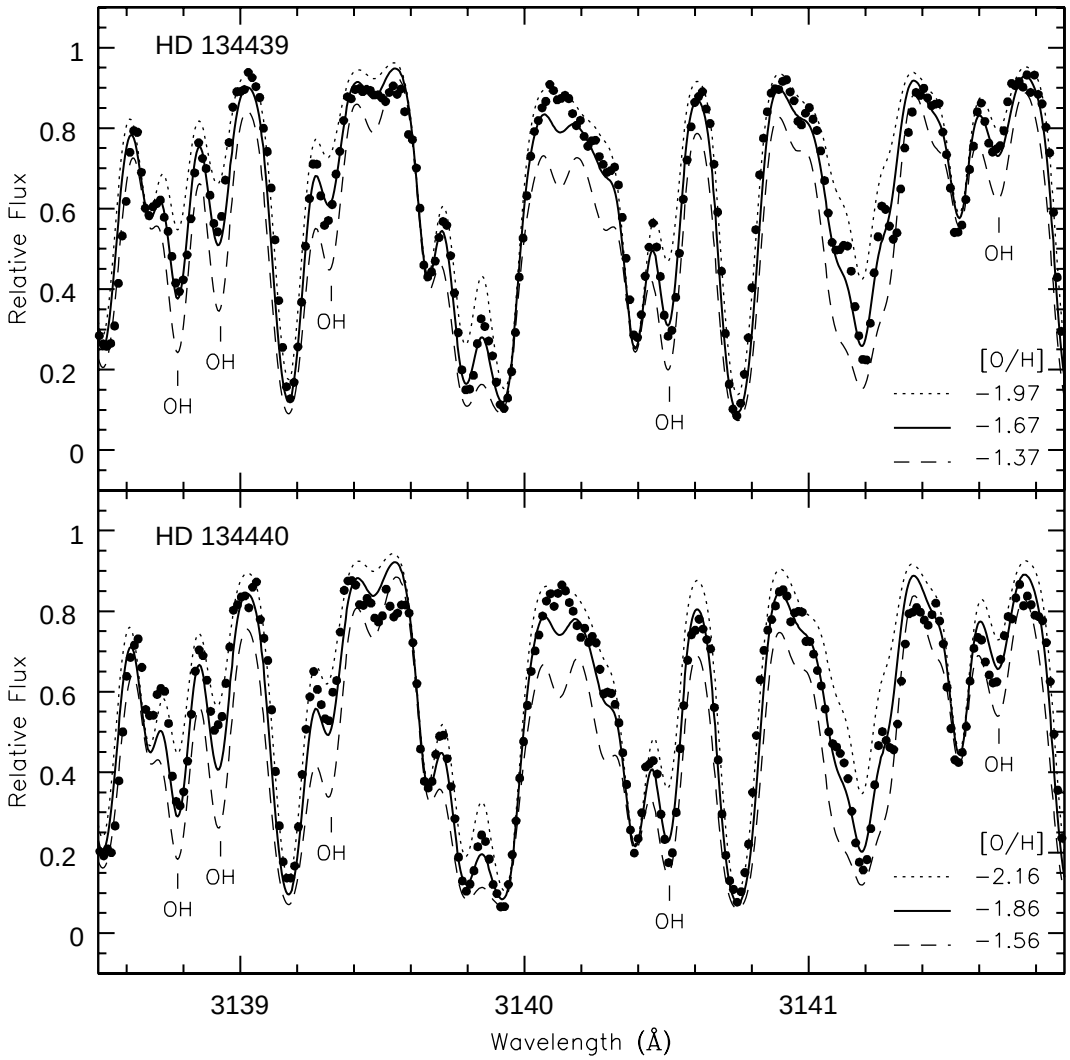

Figure A.3 Synthesis of OH molecular lines for HD 134439 (upper panel) and HD 134440 (lower panel). Filled circles indicate observed spectra. The solid line is the average best-fit [O/H] abundance by χ^2-test on all the OH lines considered. Dotted and dashed lines are ± 0.30 dex deviations from the best-fit abundance.

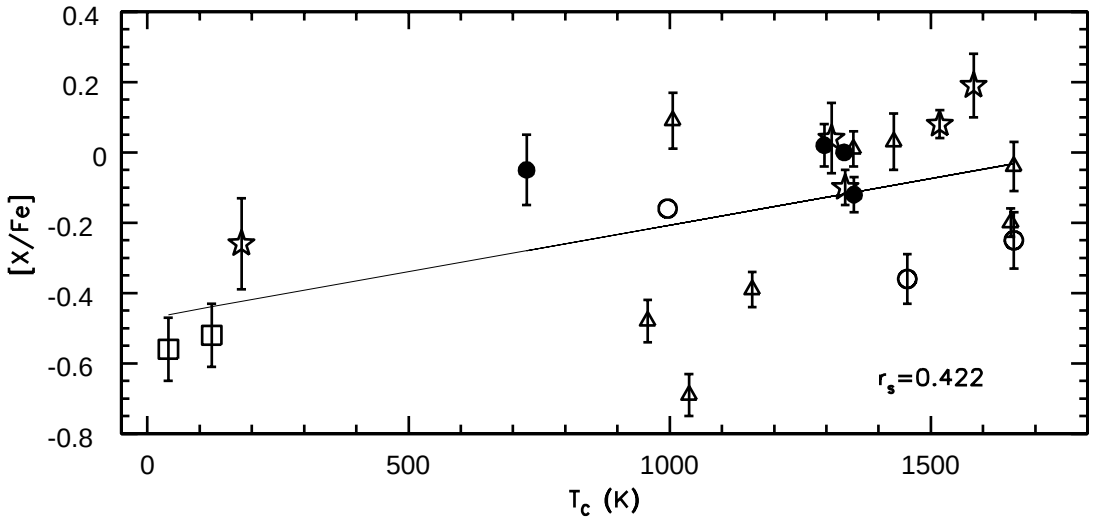

Figure A.4 Mean [X/Fe] ratios of HD 134439 and HD 134440, for the 22 elements in Table A.7, plotted against T_c. The star symbols indicate α elements, triangles are for odd iron group elements, filled circles are for even iron group elements, open circles are for n-capture elements, and open squares are for carbon and nitrogen. One σ error bars for the mean abundance ratios are shown. The least square fit to the data is shown by the solid line with a Spearman's rank correlation coefficient of 0.414.

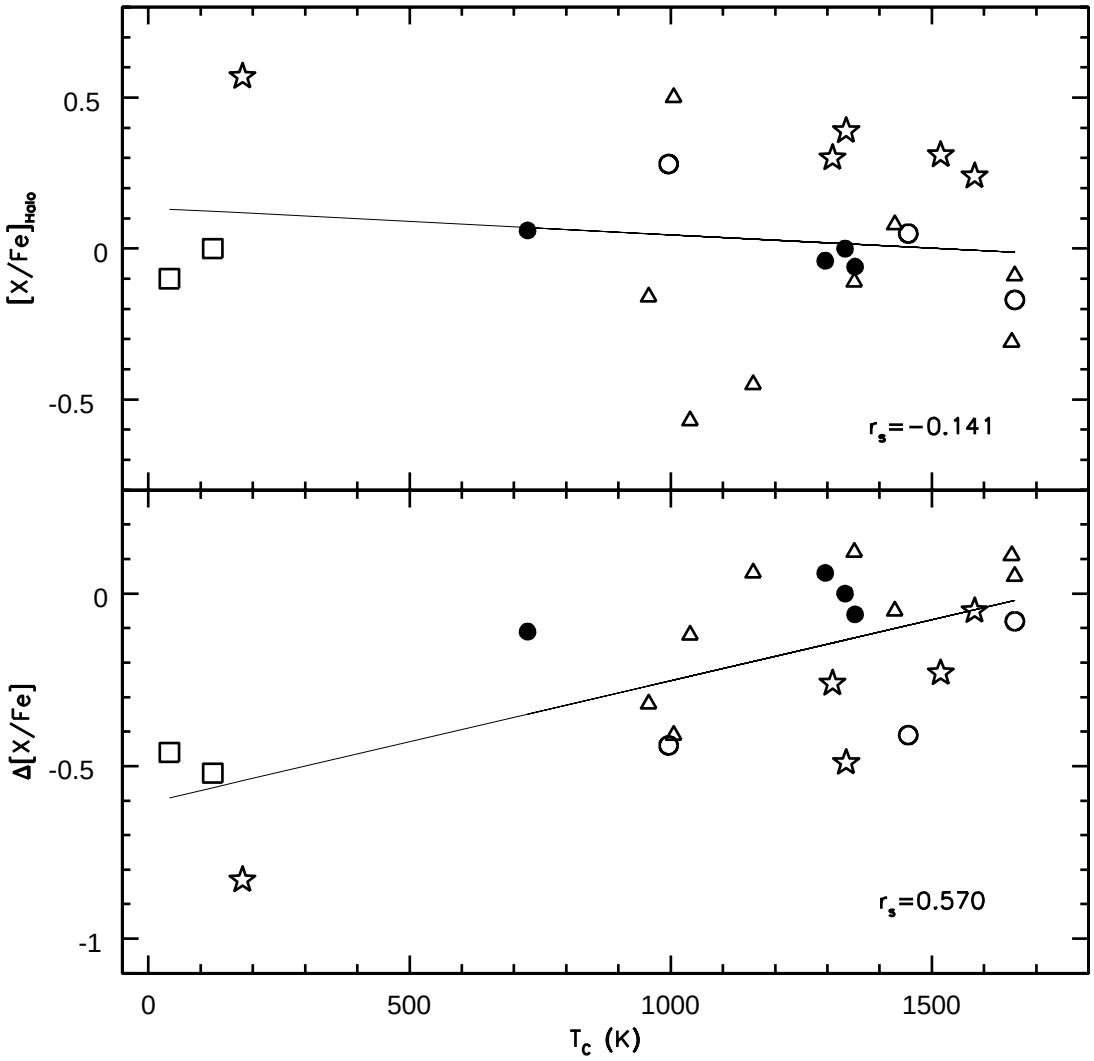

Figure A.5 Mean [X/Fe] ratios for Galactic halo stars at [Fe/H]$\sim$ 1.50 are plotted against T_c on the upper panel. Lower panel shows the deviations of mean galactic halo [X/Fe] ratios from HD 134439 and 134440 [X/Fe] ratios. The elements correspond to those in Figure A.4. Mean [Al/Fe] and [K/Fe] ratios for halo stars are adapted from Timmes et al. (1995); [Y/Fe] and [Ba/Fe] ratios are from Travaglio et al. (2004a); [Ag/Fe] for HD 103095 is from Crawford et al. (1998); [N/Fe] is assumed to be 0.0 dex (e.g., Spite et al. 2005, Israelian et al. 2004); all other [X/Fe] ratios are from Figure 28 of Kobayashi et al. (2006). The least square fit to the data is shown by the solid lines with Spearman's rank correlation coefficients of -0.106 and 0.531.

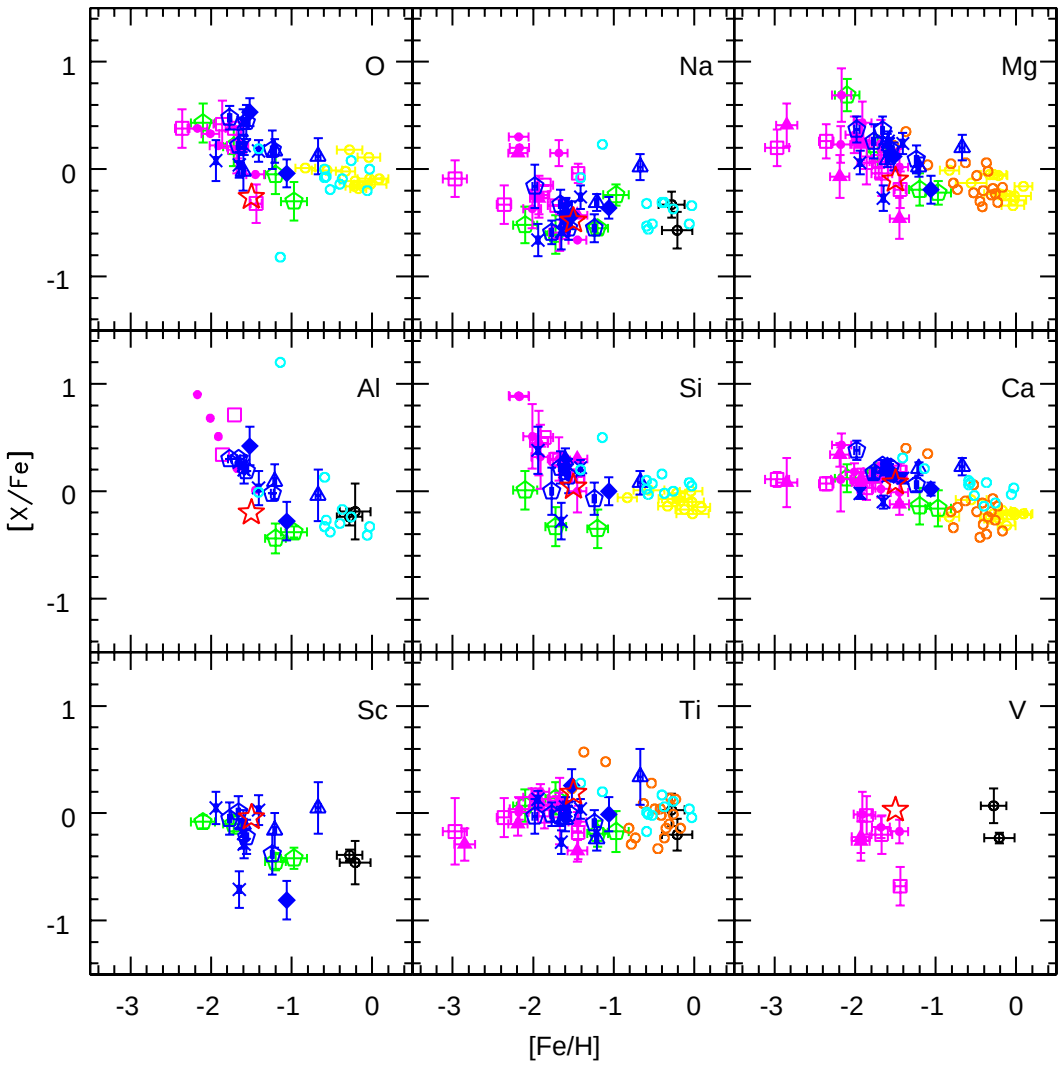

Figure A.6 [X/Fe] ratios as a function [Fe/H] for stars in dSph galaxies from various studies; data from Bonifacio et al. (2000) are indicated by black symbols, Bonifacio et al. (2004) in yellow, Geisler et al. (2005) in green, Monaco et al. (2005) in orange, Shetrone et al. (2001) in magenta, Shetrone et al. (2003) in blue, and Smecker-Hane & Mc William (1999) in cyan. The dSph galaxies are shown in different symbols; open circles for Sgr dSph, open pentagons for Scl dSph, open squares for Dra dSph, open triangles for For dSph, filled circles for UMi dSph, filled triangles for Sex dSph, filled diamonds for Leo dSph, and crosses for Car dSph. The red star symbols indicate the mean [X/Fe] ratios for HD 134439 and HD 134440. The least square fit to the data is shown by the solid lines with Spearman's rank correlation coefficients of 0.115 and 0.278.

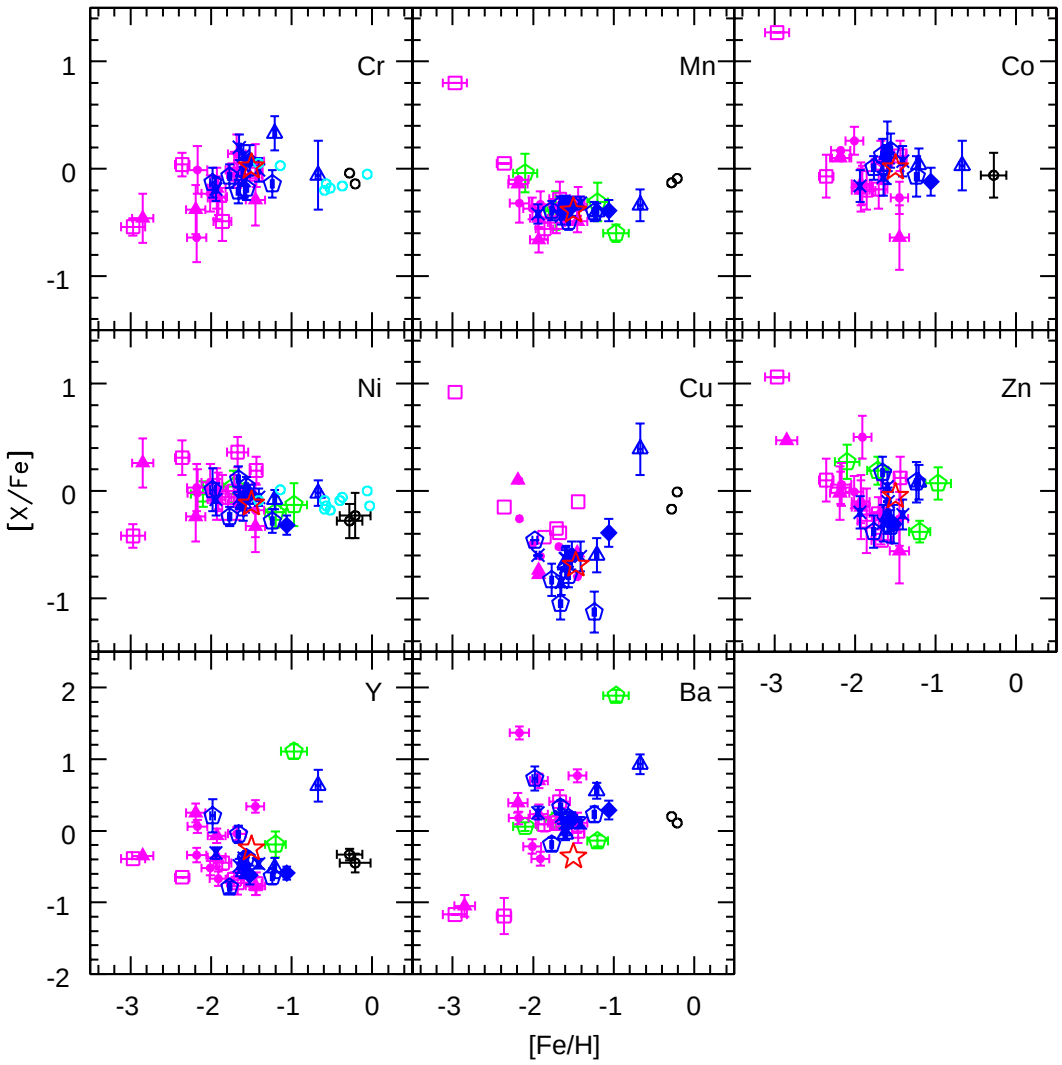

Figure A.7 Same as Figure A.6.

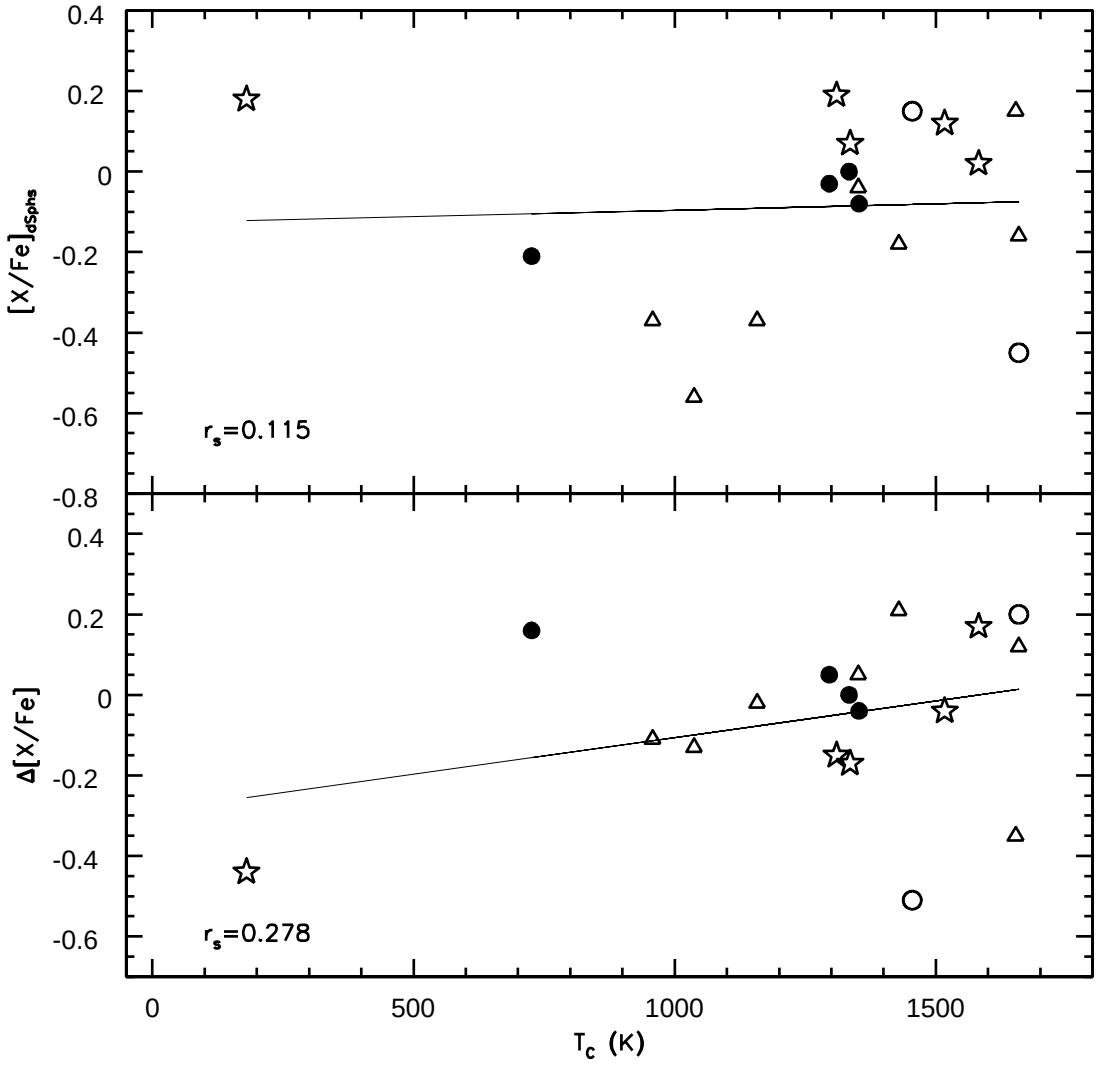

Figure A.8 Same as Figure A.5 but with mean [X/Fe] ratios for dSph stars at [Fe/H]$\sim$ 1.50. The mean values are estimated from Figure A.6 and A.7.

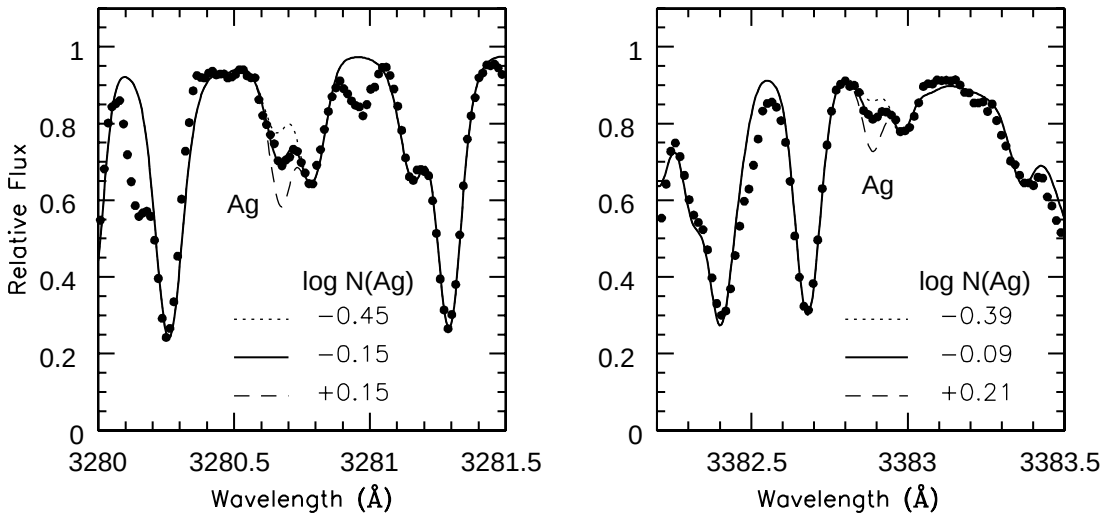

Figure A.9 Syntheses of Ag features at 3280Å (left panel) and 3382Å (right panel) for HD 134439. Filled circles indicate observed spectra. Solid line is the best estimate for Ag abundance. Dotted and dashed lines are ±0.30 dex deviations from the estimated abundance.

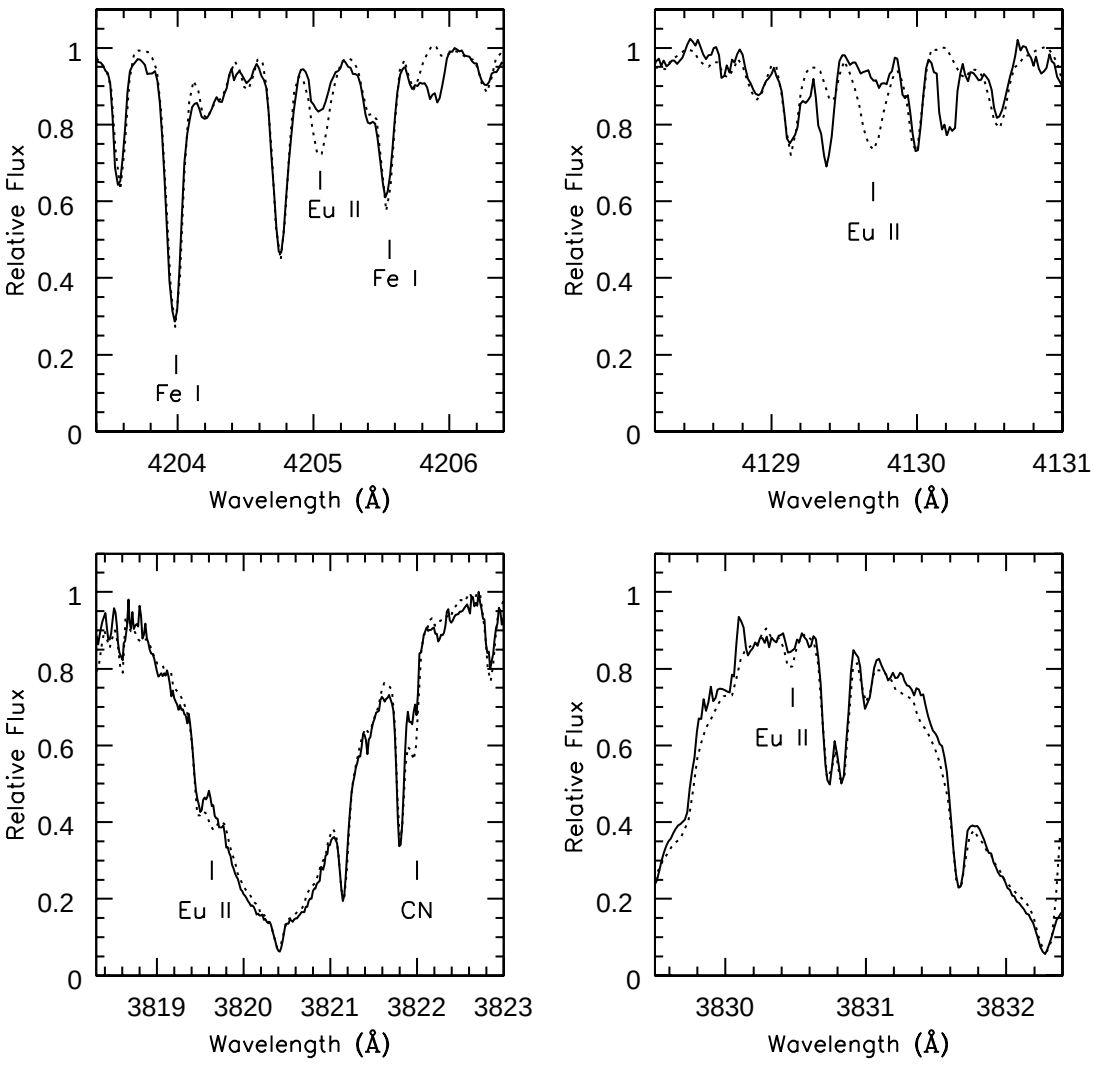

Figure A.10 A comparison of observed spectra for HD 134439 (solid line) nd HD 103095 (dotted line). The "line" near 4130.2Å is believed to be an artifact in the spectra for HD 134439 since it is not visible in the other spectral order or in HD 134440. The feature near 4129.4Å, however, appears real. Yb II lines are in our VALD list at this wavelength, but we do not observe what should be stronger known Yb features at other wavelengths.

Appendix B

Additional NH, OH, and Ag Syntheses

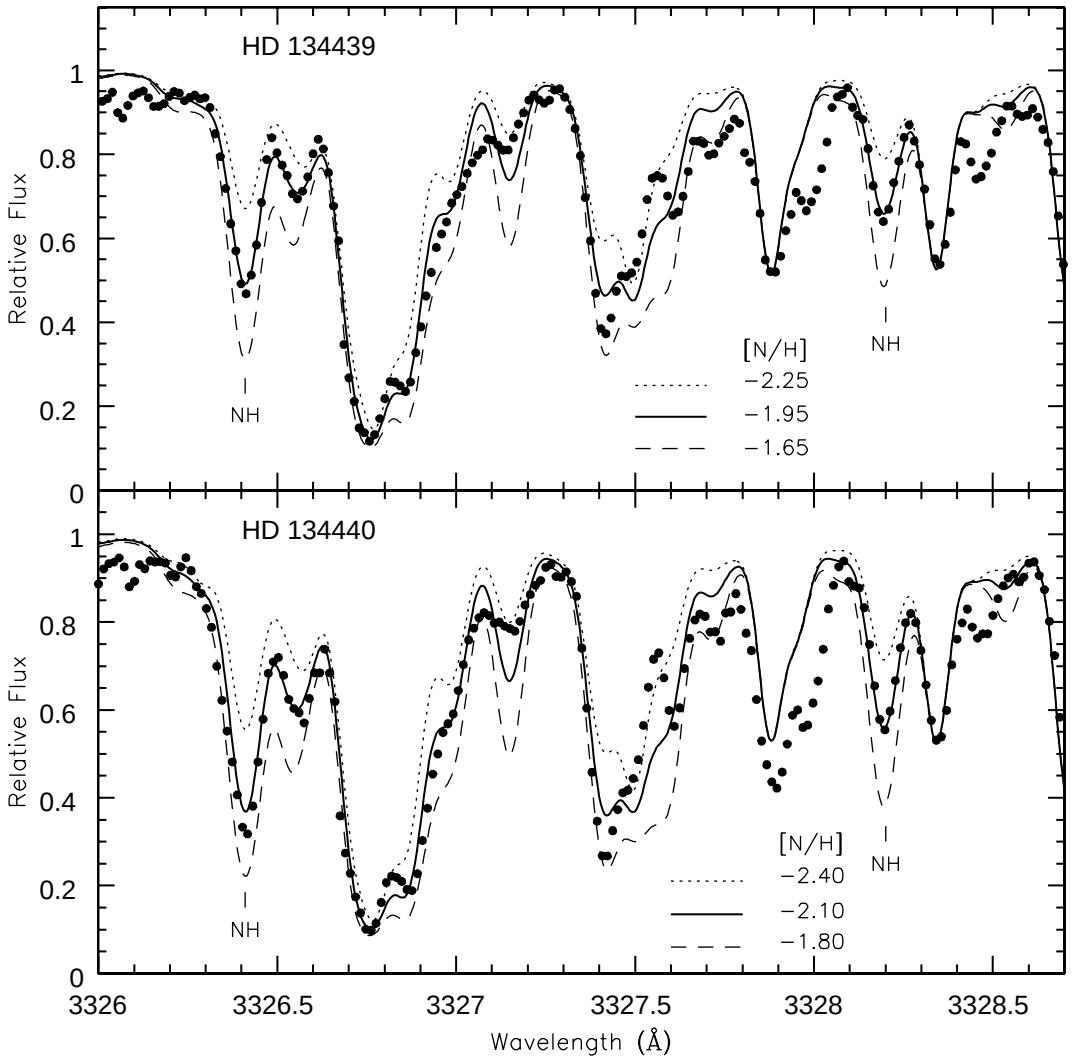

Figure B.1 Synthesis of NH molecular lines for HD 134439 (upper panel) and HD 134440 (lower panel). Filled circles indicate observed spectra. The solid line is the average best-fit [N/H] abundance by χ^2-test on the individual NH lines indicated. Dotted and dashed lines are ± 0.30 dex deviations from the best-fit abundance.

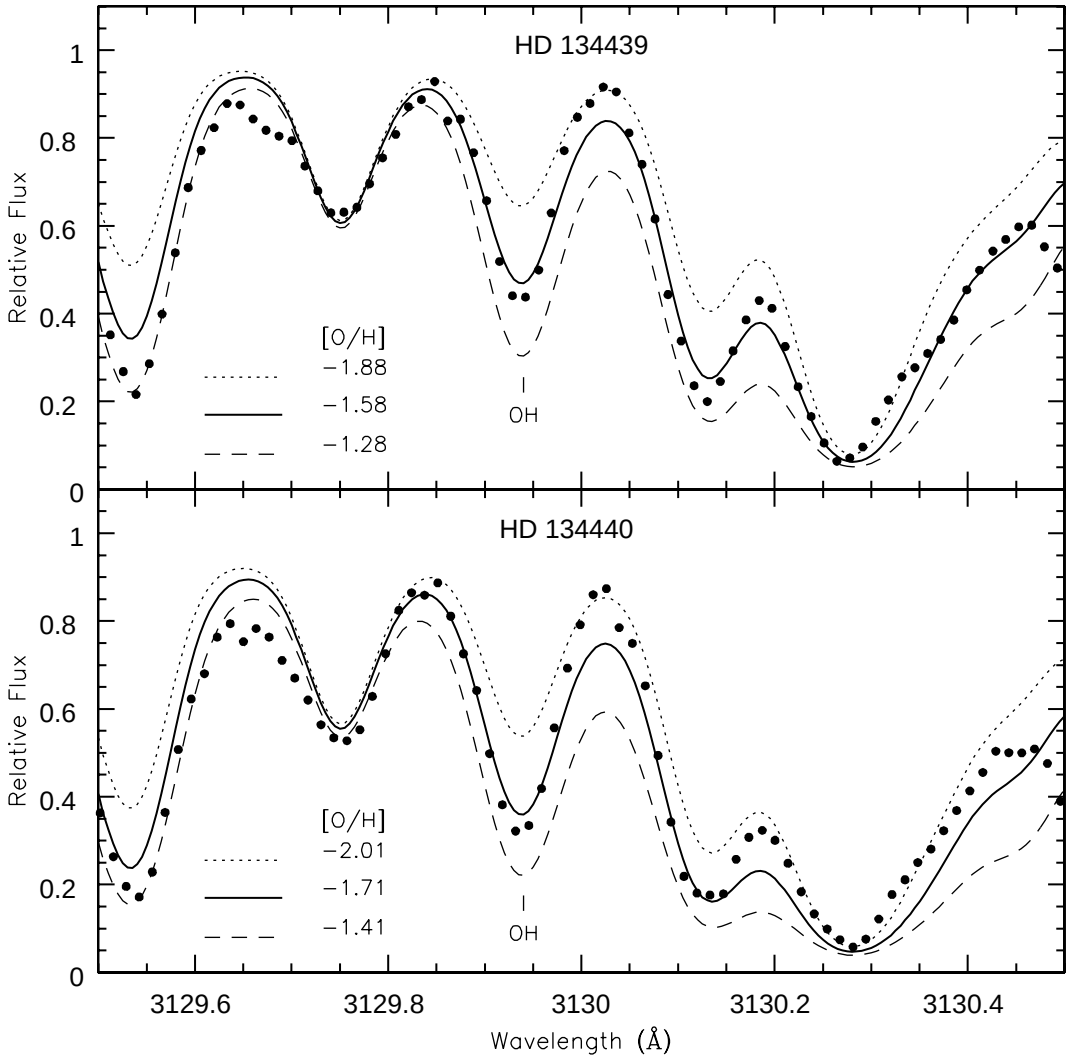

Figure B.2 Synthesis of OH molecular line for HD 134439 (upper panel) and HD 134440 (lower panel). Filled circles indicate observed spectra. The solid line is the best-fit [O/H] abundance by a χ^2-test on the OH line indicated. Dotted and dashed lines are ± 0.30 dex deviations from the best-fit abundance.

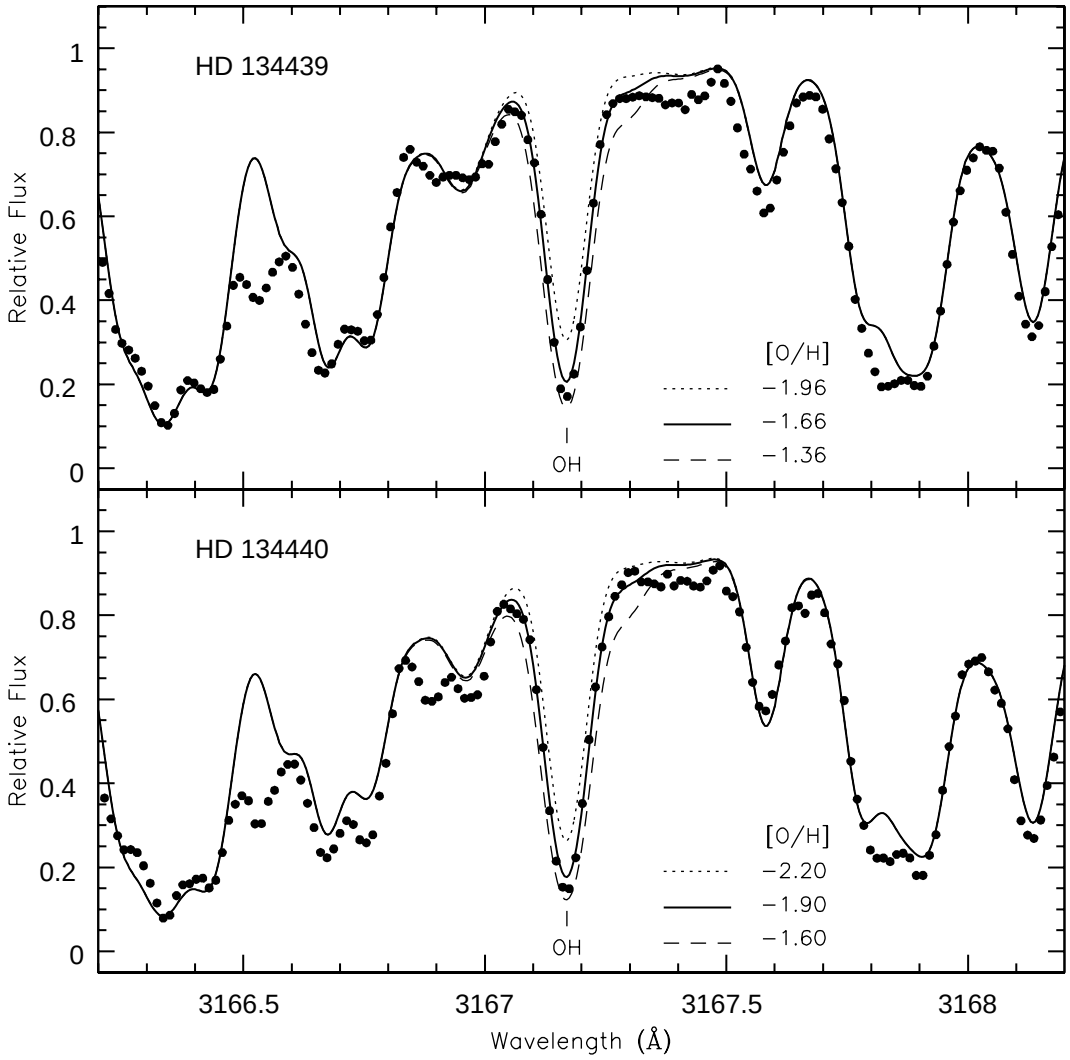

Figure B.3 Synthesis of OH molecular line for HD 134439 (upper panel) and HD 134440 (lower panel). Filled circles indicate observed spectra. The solid line is the best-fit [O/H] abundance by a χ^2-test on the OH line indicated. Dotted and dashed lines are ±0.30 dex deviations from the best-fit abundance.

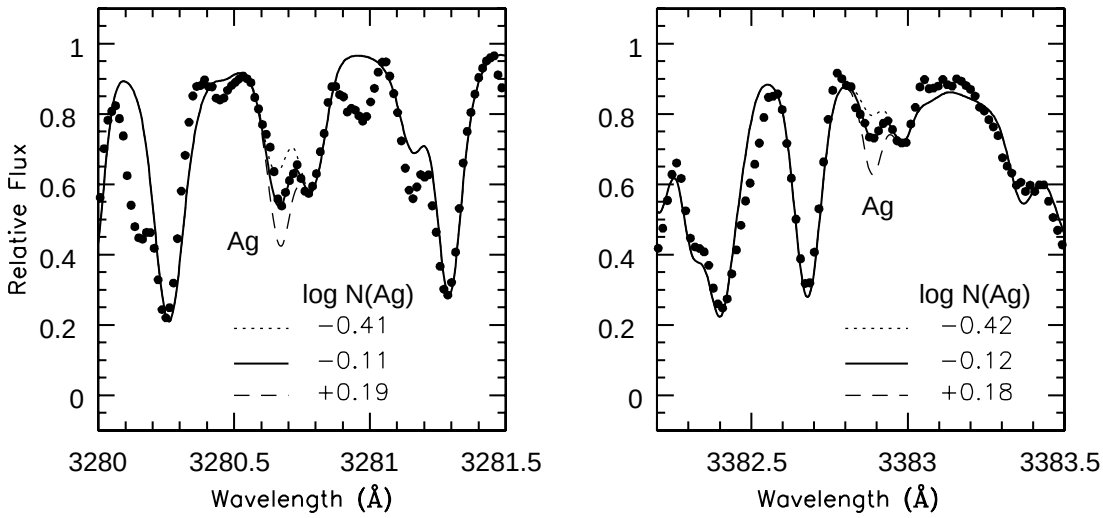

Figure B.4 Syntheses of Ag features at 3280Å (left panel) and 3382Å (right panel) for HD 134440. Filled circles indicate observed spectra. Solid line is the best estimate for Ag abundance. Dotted and dashed lines are ±0.30 dex deviations from the estimated abundance.

Bibliography

Chen, Y. Q., & Zhao, G. 2006, MNRAS, 370, 2091

Eggen, O. J., Lynden-Bell, D., & Sandage, A. R. 1962, ApJ, 136, 748

Käppeler, F., Beer, H., & Wisshak, K. 1989, Reports of Progress in Physics, 52, 945

Matteucci, F. 2008a, ArXiv e-prints, 803, arXiv:0803.3016

Matteucci, F. 2008b, ArXiv e-prints, 804, arXiv:0804.1492

Meyer, B. S. 1994, ARA&A, 32, 153

Qian, Y.-Z., & Wasserburg, G. J. 2001, ApJ, 559, 925

Shigeyama, T., & Tsujimoto, T. 2003, ApJ, 598, L47

Twarog, B. A. 1980, ApJ, 242, 242

Woosley, S. E., & Hoffman, R. D. 1992, ApJ, 395, 202